








TRIM33 drives prostate tumor growth by stabilizing androgen receptor from Skp2-mediated degradation

Mi Chen^{1,2,3,4,†} , Shreyas Lingadahalli^{1,2,3,4,†,‡} , Nitin Narwade^{1,2,3,4,†} , Kate Man Kei Lei^{1,2,3,5,6}, Shanshan Liu⁷ , Zuxianglan Zhao^{1,2,3,4}, Yimin Zheng^{1,2,3,4} , Qian Lu⁷, Alexander Hin Ning Tang⁸, Terence Chuen Wai Poon^{1,2,3,4,5,6}  & Edwin Cheung^{1,2,3,4,*} 

Abstract

Androgen receptor (AR) is a master transcription factor that drives prostate cancer (PCa) development and progression. Alterations in the expression or activity of AR coregulators significantly impact the outcome of the disease. Using a proteomics approach, we identified the tripartite motif-containing 33 (TRIM33) as a novel transcriptional coactivator of AR. We demonstrate that TRIM33 facilitates AR chromatin binding to directly regulate a transcription program that promotes PCa progression. TRIM33 further stabilizes AR by protecting it from Skp2-mediated ubiquitination and proteasomal degradation. We also show that TRIM33 is essential for PCa tumor growth by avoiding cell-cycle arrest and apoptosis, and TRIM33 knockdown sensitizes PCa cells to AR antagonists. In clinical analyses, we find TRIM33 upregulated in multiple PCa patient cohorts. Finally, we uncover an AR-TRIM33-coactivated gene signature highly expressed in PCa tumors and predict disease recurrence. Overall, our results reveal that TRIM33 is an oncogenic AR coactivator in PCa and a potential therapeutic target for PCa treatment.

Keywords androgen signaling; prostate cancer; transcriptional regulation; TRIM33

Subject Categories Cancer; Chromatin, Transcription, & Genomics; Post-translational Modifications & Proteolysis

DOI 10.15252/embr.202153468 | Received 17 June 2021 | Revised 13 May 2022 | Accepted 7 June 2022 | Published online 4 July 2022

EMBO Reports (2022) 23: e53468

Introduction

Prostate cancer (PCa) is the most common noncutaneous cancer and is responsible for the second-highest cancer-related death among men (Siegel *et al*, 2020). Androgen receptor (AR) occupies a central position in the development and progression of PCa (Heemers & Tindall, 2009; Massie *et al*, 2011). Thus, androgen deprivation therapy (ADT) has been widely used as the primary treatment for advanced PCa (Miller *et al*, 2019). While patients demonstrate a favorable initial response to ADT, in most cases, the disease will inevitably recur and progress to a fatal stage of PCa termed castration-resistant prostate cancer (CRPC), which is also driven by AR signaling (Feldman & Feldman, 2001; Decker *et al*, 2012; Grasso *et al*, 2015).

After activation by androgen, AR translocates to the nucleus, binds to specific AR binding sites (ARBBS), and recruits multiple coregulators in a highly regulated manner (Bennett *et al*, 2010). These coregulators then form a productive AR transcriptional complex that ultimately determines the transcriptional outcome of AR. Coregulators act at the promoter and enhancer regions of AR target genes and display vital roles in controlling the AR-mediated transcription process through specific and distinct ways (Heemers & Tindall, 2007; Sung & Cheung, 2014). Androgen receptor coregulators are divided into four main types based on their functional characteristics: (i) pioneer factors (e.g., FOXA1) bind to chromatin before androgen stimulation to modulate AR genome occupancy; (ii) collaborative factors (e.g., ERG) facilitate AR binding by recruiting other cofactors to modify the epigenetic state of the surrounding chromatin; (iii) coactivators (e.g., p160/SRC) enhance AR transcriptional activity by acting as bridging factors or chromatin modifiers;

1 Cancer Centre, University of Macau, Taipa, Macau SAR
 2 Centre for Precision Medicine Research and Training, University of Macau, Taipa, Macau SAR
 3 MoE Frontiers Science Center for Precision Oncology, University of Macau, Taipa, Macau SAR
 4 Faculty of Health Sciences, University of Macau, Taipa, Macau SAR
 5 Pilot Laboratory, University of Macau, Taipa, Macau SAR
 6 Institute of Translational Medicine, University of Macau, Taipa, Macau SAR
 7 Xuzhou Medical University, Xuzhou, China
 8 Department of Pathology, The University of Hong Kong, Hong Kong, Hong Kong SAR
 *Corresponding author. Tel: +853 88224992; E-mail: echeung@um.edu.mo
 †These authors contributed equally to this work
 ‡Present address: Vancouver Prostate Centre, Vancouver, BC, Canada

and (iv) corepressors (e.g., NCoRs) suppress AR transcriptional activity (Sung & Cheung, 2014).

The importance of coregulators in defining the AR transcription output implies a critical role for these regulatory proteins in pathologies linked to aberrant AR action, such as PCa. Indeed, accumulating evidence shows that aberrant expression or improper regulation of these coregulators alter the AR transcriptional landscape, promoting PCa tumorigenesis and progression (Wang *et al*, 2009; Sharma *et al*, 2013; Mills, 2014; Pomerantz *et al*, 2015). Hence, identifying all the essential components of the AR coregulator complex is necessary for understanding the molecular mechanism of androgen-regulated transcription and discovering new promising pharmacological targets in this pathway.

In this study, we utilized a proteomics approach called rapid immunoprecipitation of endogenous proteins (RIME) to systematically identify all coregulator proteins of the AR interactome in PCa cells. We functionally characterized one of these coregulators, TRIM33. We demonstrate that TRIM33 is a potent coactivator of AR transcriptional activity. Mechanistically, we show TRIM33 promotes PCa growth by preventing AR from Skp2-mediated protein degradation. Finally, we identified an AR-TRIM33 coregulatory gene signature that is overexpressed in PCa, essential for disease progression, and predicts recurrence-free survival.

Results

TRIM33 is a novel AR-interacting protein

To obtain an unbiased and comprehensive catalog of AR-interacting proteins in PCa, we performed a series of RIME analyses (Mohammed *et al*, 2016) with anti-AR antibody and IgG (control) on dihydrotestosterone (DHT)-stimulated LNCaP and VCaP cells. We determined high confident AR interactors by applying the following stringent criteria: (i) interacting proteins are present in three biological replicates, (ii) for each interacting protein, the ratio of normalized label-free quantification (LFQ) intensity between the AR pull-down and the IgG pull-down > 5, and (iii) the number of unique peptides representing each interacting protein in the AR pull-down > 4. Based on these criteria, we identified 134 and 177 AR-interacting proteins in LNCaP and VCaP cells, respectively (Dataset EV1). Overlapping the AR-interacting proteins from LNCaP and VCaP cells revealed 91 common proteins between the two cell lines (Fig EV1 and Dataset EV1). When we categorized the AR-interacting proteins according to their biological processes, we found they are enriched for functional roles such as DNA binding, chromatin binding, RNA binding, and enzyme binding (Fig 1A). Our AR-RIME on PCa cells captured many well-characterized AR

coactivators (e.g., EP300, NCOAs, and PARP1), corepressors (e.g., NCoRI, SMRT, and HDACs), and components of the large chromatin-modifying complex SWI/SNF (e.g., SMCA5, SMARCB1, SMARCD2, and SMARCC2; Sung & Cheung, 2014). We also found numerous AR collaborative factors, including NKX3-1, HOXB13, GRHL2, and pioneer factors FOXA1 and GATA2 (Sung & Cheung, 2014). While we were able to identify many known components of the AR coregulatory complex, approximately 50% of the hits from our RIME analysis are novel AR-interacting proteins. Among the top-ranked hits that appear in both LNCaP and VCaP cells is TRIM33 (Fig 1A and B), a member of the tripartite motif-containing family of proteins involved in transcriptional regulation, cell growth, and tumorigenesis (Hatakeyama, 2011). We validated the association between AR and TRIM33 in coimmunoprecipitation assays (Fig 1C). We also performed *in vitro* GST pull-down assays with bacterially expressed and purified proteins, GST-AR immobilized to GSH beads, and his-MBP-TRIM33. Our results show that immobilized GST-AR could pull down his-MBP-TRIM33, suggesting AR interacts with TRIM33 directly (Fig 1D).

An interplay between AR and TRIM33 cistromes in androgen signaling

To begin determining whether TRIM33 is a coregulator of AR in androgen-dependent transcription, we first asked whether TRIM33 is recruited to AR binding sites (ARBSS). To do this, we performed ChIP-seq of TRIM33 in LNCaP cells. Overall, we identified 7,532 and 12,431 TRIM33 binding sites (T33BSs) before and after DHT treatment, respectively (Fig 2A). Besides increasing the number of T33BS, DHT also enhanced the average binding intensity of TRIM33 (Fig 2B). By overlapping the T33BSs with ARBSs from our previous AR ChIP-seq dataset (Tan *et al*, 2012), we identified 3,067 AR-TRIM33 colocalized binding sites (Fig EV2A). TRIM33 binding intensity at colocalized sites was also enhanced upon DHT stimulation (Fig 2C). Similar to the genomic distribution profile of AR (Tan *et al*, 2012), AR and TRIM33 are mainly co-occupied in distal intergenic and intronic regions (Fig 2D). Moreover, motif analysis of the AR-TRIM33 shared cistrome revealed significant enrichment for the AR binding motif (ARE; Fig 2E), suggesting TRIM33 is recruited to these binding sites by AR. To determine whether TRIM33 potentially plays a role in AR-dependent transcription, we searched for TRIM33 binding at ARBSs associated with model androgen-regulated genes. As shown in Fig 2F and G, DHT strongly stimulated TRIM33 binding at ARBSs of KLK2, KLK3, and FKBP5. Moreover, depleting AR abolished TRIM33 binding at these ARBSs without affecting TRIM33 protein level (Figs 2G and EV2B), further supporting that AR recruits TRIM33. Together, our results suggest an interplay between the AR and TRIM33 cistromes in androgen-regulated transcription.

Figure 1. TRIM33 is a novel protein interactor of AR.

- MS-ARC graphs showing AR-associated proteins with DHT stimulation in LNCaP cells (left) and VCaP cells (right). The proteins were clustered according to their molecular function. The length of each line represents the ratio of normalized LFQ intensity between the AR pull-down and the IgG pull-down.
- Peptide coverage of TRIM33 for the corresponding RIME experiment.
- Validation of the AR and TRIM33 interaction by coimmunoprecipitation assays. Endogenous AR protein in LNCaP cells (left) or VCaP cells (right) were immunoprecipitated and detected for TRIM33 by immunoblotting. IgG served as a negative control.
- In vitro* GST pull-down assays were performed with bacterially expressed and purified GST or GST-tagged AR immobilized onto GSH beads. Immobilized GST protein beads were used to pull down purified his-MBP (left) or his-MBP-tagged TRIM33 (right).

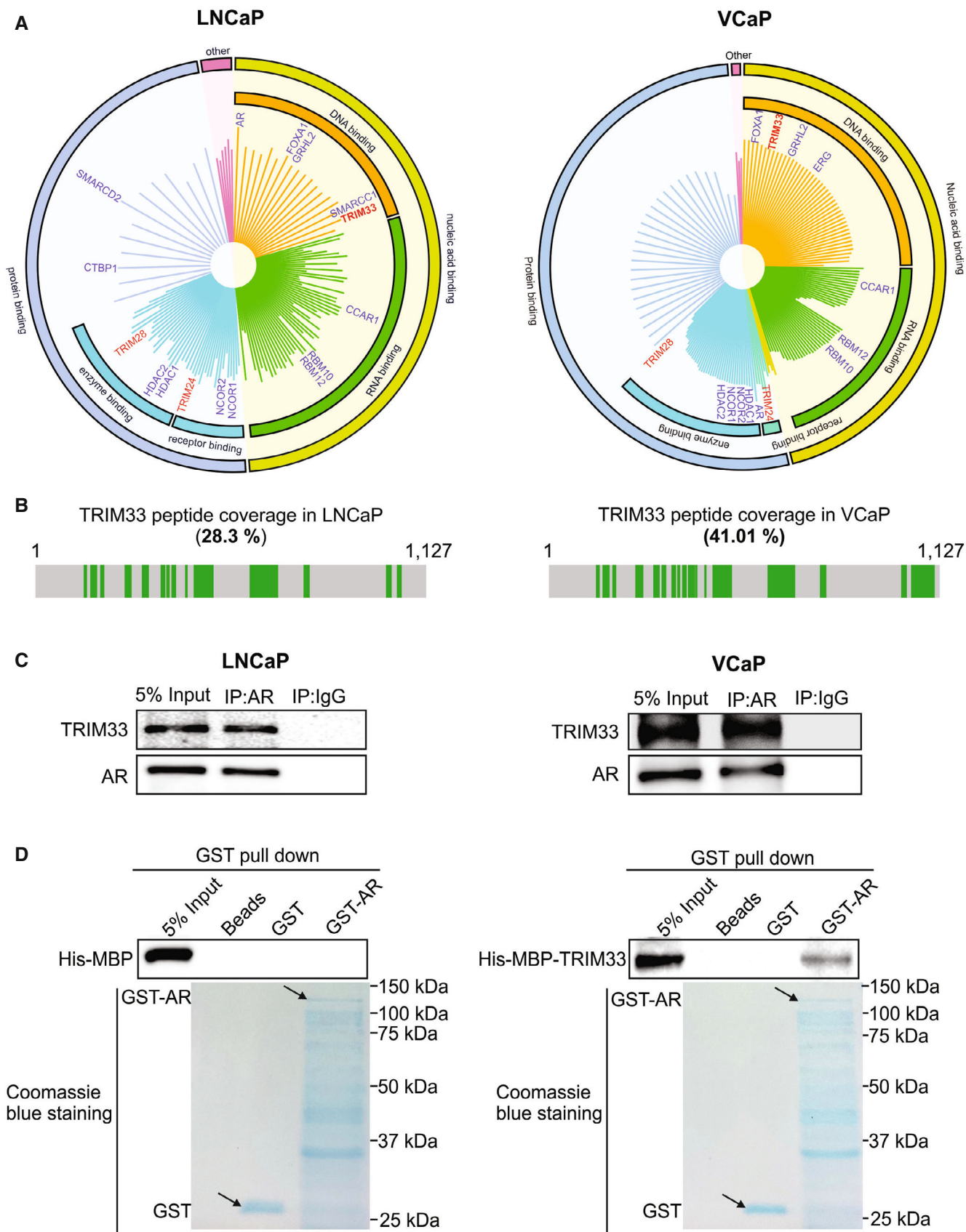


Figure 1.

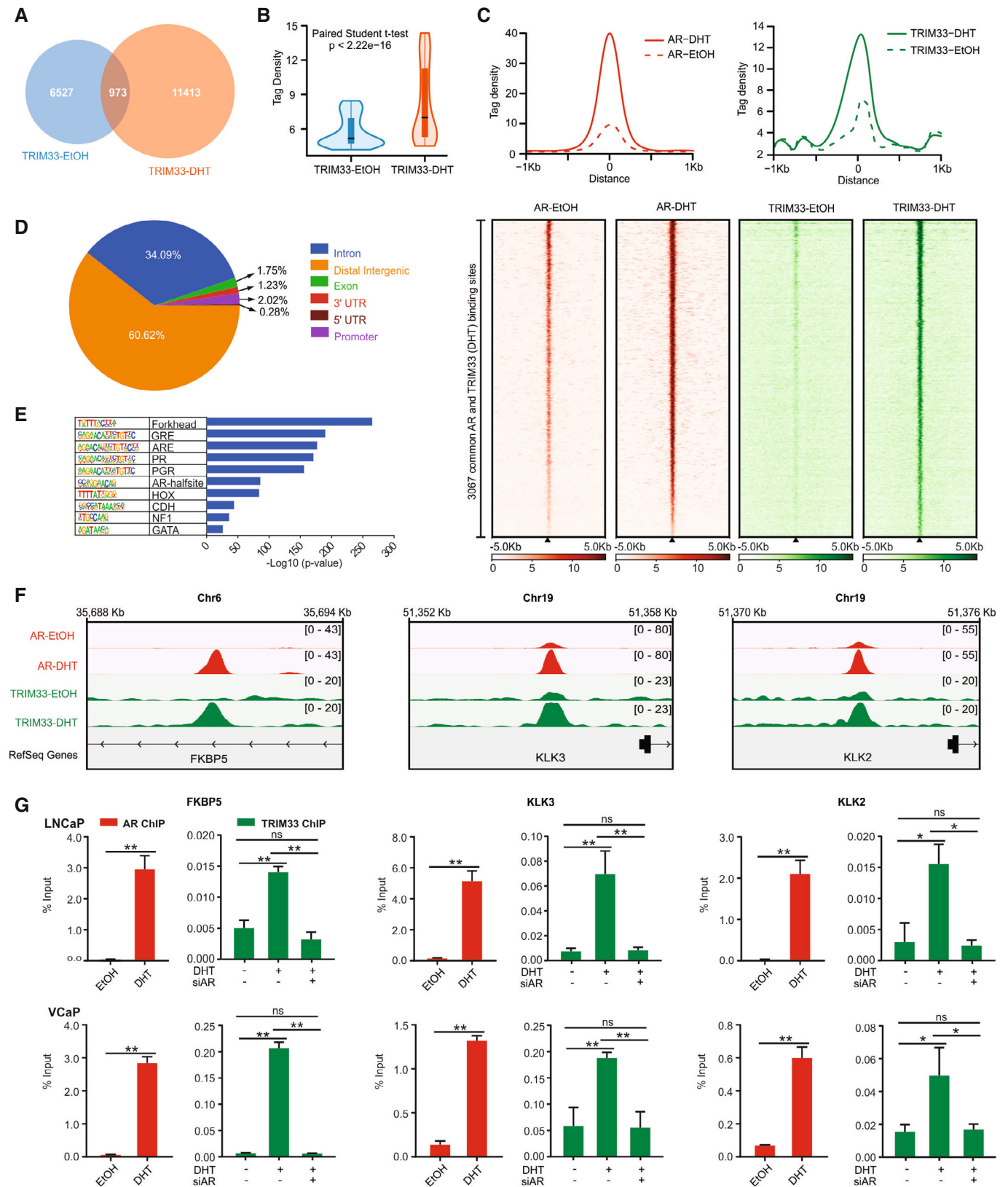


Figure 2. The interplay between TRIM33 and AR cistromes in PCa.

- A Venn diagram overlapping EtOH- and DHT-treated TRIM33 cistromes in LNCaP cells.
- B Comparison between tag densities of TRIM33-binding sites (T33BSs) from EtOH- and DHT-treated LNCaP cells. The tag density distribution is represented in the form of a violin plot. The inner boxplot shows the first and third quartiles and is split by the medians, whiskers extending a 1.5-fold interquartile range beyond the box.
- C Average tag densities of AR (left) and TRIM33 (right) binding at 3,067 shared binding sites from EtOH- and DHT-treated LNCaP cells (upper panel). Heatmaps show AR (left) and TRIM33 (right) normalized binding intensity at shared binding sites (lower panel).
- D Pie chart illustrating the genomic distribution of AR-TRIM33 shared binding sites on chromatin. The assessed binding distribution included intron, distal intergenic, exon, 5' and 3' UTRs, and promoter regions.
- E Top motifs enriched from DHT-treated AR-TRIM33 shared peaks. *P*-values for enrichment over genomic background are shown.
- F Genomic snapshots of AR and TRIM33 ChIP-seq peaks surrounding FKBP5, KLK3, and KLK2.
- G Bar graphs showing the ChIP-qPCR results of AR and TRIM33 binding at FKBP5, KLK3, and KLK2 in LNCaP (top) and VCaP (bottom) cells with or without transient AR knockdown. The data are represented as a percentage of input chromatin immunoprecipitated.
- Data information: In (G), data are presented as mean \pm SD ($n = 3$ independent experiments); * $P < 0.05$; ** $P < 0.01$; ns = not significant (two-way ANOVA).

TRIM33 is a coactivator of the AR transcriptional program

Since TRIM33 interacts with AR and both factors are colocalized on chromatin, we next examined whether TRIM33 acts as a positive or negative coregulator of AR transcriptional activity. To do this, we performed luciferase reporter assays on LNCaP cells in which we depleted or overexpressed TRIM33 together with a luciferase reporter construct containing AR responsive elements upstream of a minimal TATA box. TRIM33 depletion significantly reduced AR transcriptional activity (Fig 3A), while overexpression led to a concentration-dependent increase in AR activity (Fig 3B). Moreover, depleting AR abrogated the positive transcriptional effect of TRIM33 (Fig 3C). We also assessed the effect of TRIM33 on endogenous androgen-regulated genes. Consistent with the transient transfection results, silencing TRIM33 reduced the expression of KLK2, KLK3, and FKBP5 in LNCaP and VCaP cells (Fig 3D), while overexpressing TRIM33 had the opposite effect (Fig 3E). Together, these findings suggest TRIM33 is a coactivator of AR-dependent transcription in PCa cells.

To determine the extent of TRIM33 coactivator activity on the global AR transcriptional program in PCa cells, we performed RNA-seq analysis on DHT-stimulated LNCaP cells with or without TRIM33 depletion. Overall, we identified 3,516 TRIM33 responsive genes (1,623 up and 1,893 down; Dataset EV2). We found that TRIM33-regulated genes are significantly associated with TRIM33 binding (Fig EV3A), suggesting TRIM33 can directly regulate transcription in PCa cells. We also examined TRIM33-regulated genes together with DHT-regulated genes (1,240 up and 1,249 down, Dataset EV3). In gene set enrichment analyses (GSEA), androgen-induced genes are significantly enriched in genes downregulated by siTRIM33, while androgen-repressed genes are highly enriched in genes de-repressed by siTRIM33 (Fig 3F). These results are consistent with the above transient analyses and further support TRIM33 as an AR coactivator.

Next, we investigated the biological function of the AR-TRIM33 coregulated transcriptional program in PCa. Of the 1,240 DHT-upregulated genes, 414 were suppressed by TRIM33 depletion, including model AR-regulated genes, such as KLK2, KLK3, and FKBP5 (Fig 3G and Dataset EV4). As for the 1,249 DHT-downregulated genes, 536 were de-repressed by TRIM33 depletion (Fig 3G and Dataset EV4). In addition, we found that AR-TRIM33-coactivated but not corepressed genes are significantly associated with AR and TRIM33 cobinding, suggesting that AR and TRIM33 collaboration preferentially activate transcription (Fig EV3B). Functional enrichment analyses of the AR-TRIM33-coactivated genes

show significant enrichment for biological processes associated with DNA metabolism, cell cycle, and cell mitosis, and pathways involved in prostate tumorigenesis (e.g., PI3K-Akt, MAPK FoxO, and ErbB signaling pathways; Fig 3H and Table EV1). In contrast, corepressed genes are enriched for biological processes related to cell proliferation and the native immune response (Appendix Fig S1 and Table EV1). Together, our results show that TRIM33 plays a critical role in shaping the AR transcriptome and suggests it promotes PCa growth by activating pro-mitotic genes.

TRIM33 facilitates AR binding to chromatin

To address the underlying mechanism of how TRIM33 upregulates the AR transcription program, we asked whether TRIM33 behaves as a coactivator by augmenting AR chromatin binding. To test this possibility, we examined the effect of global AR binding to chromatin before and after TRIM33 depletion. Our findings show that TRIM33 depletion significantly reduced the average binding intensity of AR at the 3,067 shared binding sites (Fig 4A), including the ARBSs associated with KLK2, KLK3, and FKBP5 (Fig 4B). We validated the effect of TRIM33 knockdown on ARBSs at these model genes in LNCaP and VCaP cells by ChIP-qPCR (Fig 4C). Together, these results indicate that TRIM33 is required for maximal AR chromatin binding.

TRIM33 stabilizes AR protein levels

TRIM proteins have multiple functions, including the ability to stabilize their substrates (Wei et al, 2016; Fong et al, 2018). Thus, we speculated that TRIM33 might be working as a coactivator of androgen-dependent transcription by modulating AR protein levels. We explored this hypothesis by first examining the effect of depleting or overexpressing TRIM33 on AR protein and transcript levels. TRIM33 depletion decreased full-length AR protein expression levels, while ectopic expression had the opposite effect (Figs 5A–D and EV4A–D). Under both conditions, AR mRNA levels were minimally affected (Fig 5A–D). Additionally, we found that depletion of TRIM33 also decreased the protein level of AR variant 7 (AR-V7) in VCaP cells (Fig EV4E). These results imply that TRIM33 regulates AR transcriptional activity at the post-translational level, possibly by stabilizing AR protein levels. To test whether this potential control mechanism occurs, we blocked protein translation in LNCaP cells with cycloheximide (CHX) and then assessed AR protein levels after TRIM33 depletion. Western blot analysis shows that depleting

TRIM33 significantly shortened AR protein half-life, from more than 12 h to approximately 8.5 h (Fig 5E and F). Together, these findings suggest TRIM33 is a positive regulator of AR protein stability.

Next, we asked if TRIM33 stabilizes AR protein levels by regulating the proteasomal degradation pathway. To do this, we analyzed AR protein levels on control and TRIM33 knockdown LNCaP cells

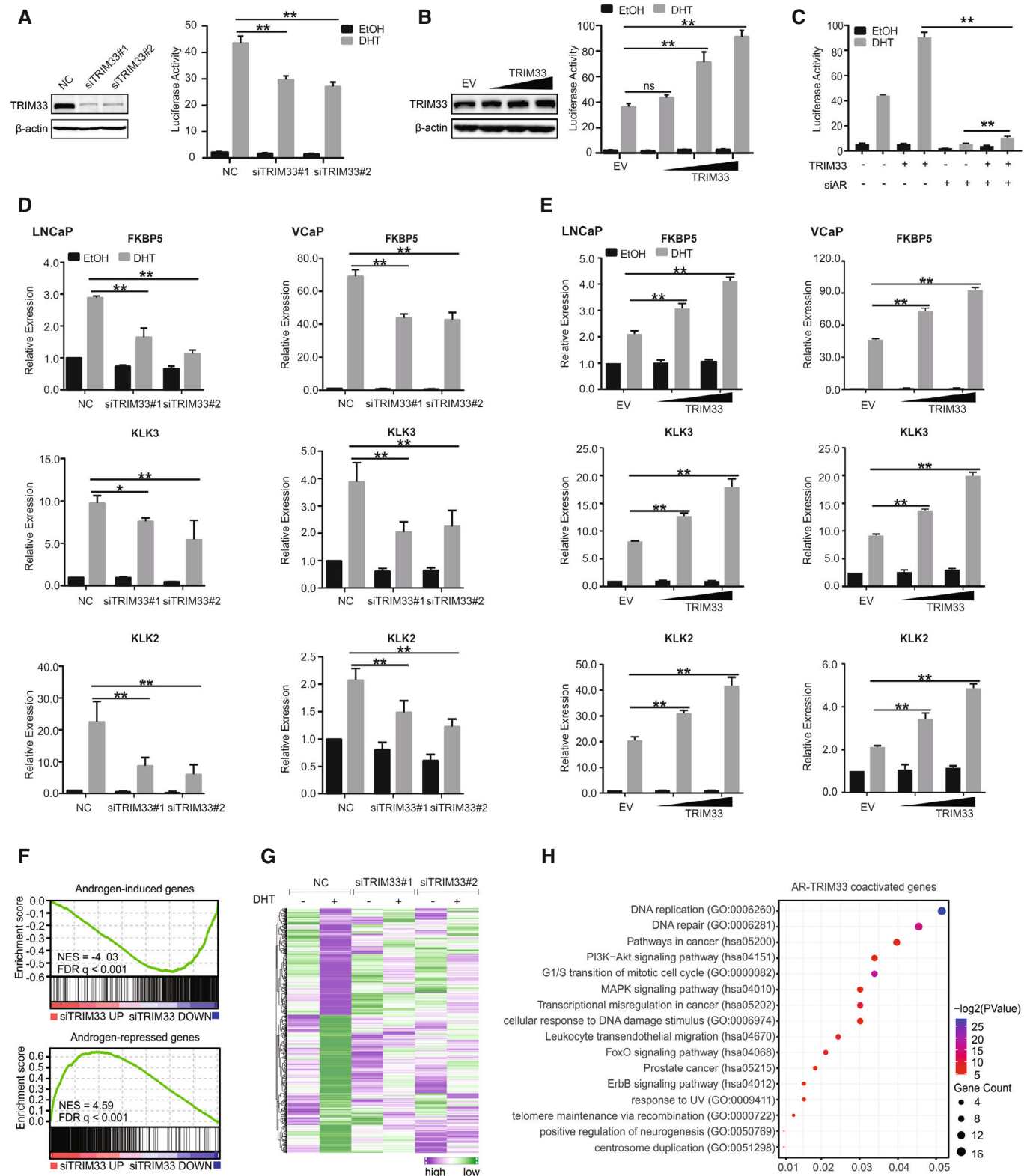


Figure 3.

Figure 3. TRIM33 enhances the AR transcriptional program.

- A–C AR-dependent luciferase assays were performed on LNCaP cells transfected with siTRIM33 or negative control (NC) (A), increasing amounts of TRIM33 plasmid (B), or TRIM33 plasmid and/or siAR (C). Western blot analysis shows the protein level of TRIM33 in LNCaP cells after TRIM33 knockdown (A) or overexpression (B).
- D LNCaP cells (left) and VCaP cells (right) were transfected with the indicated siRNAs and treated with EtOH or 10 nM DHT for 12 h. Gene expression was measured by RT-qPCR after 48 h. Data were normalized against GAPDH.
- E LNCaP (left) or VCaP (right) cells were transfected with the indicated amount of TRIM33 plasmid and treated with EtOH or 0.1 nM DHT for 12 h. Gene expression was measured by RT-qPCR after 48 h. Data were normalized against GAPDH.
- F GSEA was performed to determine the enrichment of androgen-induced (upper panel) or -repressed gene set (lower panel) in siTRIM33-regulated gene set identified by RNA-seq in LNCaP cells treated with DHT.
- G Gene expression of LNCaP cells treated with siTRIM33 or NC were profiled by RNA-seq. A total of 414 coinduced genes (androgen-induced and siTRIM33 suppressed) and 536 corepressed genes (androgen-suppressed and siTRIM33-induced) were identified and clustered across all samples.
- H Functional enrichment analysis showing the main biological processes and pathways significantly enriched by AR-TRIM33-coactivated genes ($P < 0.05$, DAVID 6.8).
- Data information: In (A–E), data are presented as mean \pm SD ($n = 3$ independent experiments); * $P < 0.05$; ** $P < 0.01$; ns = not significant (two-way ANOVA).

that have been treated with the proteasome inhibitor MG132. Our results show that MG132 abolished the repressive effect of TRIM33 depletion on AR protein levels (Fig 5G). Proteasomal degradation of a protein follows a well-defined process, including ubiquitination (Pickart, 2001). Thus, we determined whether TRIM33 stabilizes AR by preventing its ubiquitination. For this, we performed an AR ubiquitination assay on LNCaP cells depleted or overexpressed with TRIM33. As shown in Fig 5H, TRIM33 depletion increased AR ubiquitination. However, this effect on AR was overcome by the ectopic expression of TRIM33 (Fig 5I). Together, our findings indicate that TRIM33 functions as a coactivator of androgen-dependent transcription in PCa by impeding the ubiquitin-proteasome-mediated degradation of AR.

TRIM33 prevents Skp2-mediated degradation of AR

Androgen receptor is subject to ubiquitin-proteasome-mediated degradation in PCa cells by several E3 ubiquitin ligases, including SPOP and Skp2 (An *et al.*, 2014; Li *et al.*, 2014). Thus, we reasoned that TRIM33 might disrupt SPOP- or Skp2-mediated ubiquitination and degradation of AR. Consistent with previous observations, we show that both SPOP and Skp2 significantly reduced AR protein levels (Fig 5J and K). Notably, overexpressing TRIM33 rescued AR protein levels in the presence of Skp2 but not SPOP (Fig 5J and K). Moreover, loss of Skp2 restored AR protein levels in TRIM33-depleted LNCaP cells (Fig 5L). Together, these results suggest that TRIM33 stabilizes AR from Skp2-mediated degradation.

Distinct TRIM33 domains are required for blocking Skp2-mediated degradation of AR

To determine whether the physical interaction between TRIM33 and AR is required for protecting AR from degradation, we first mapped the interaction domains between the two proteins. We performed co-IP assays on 293T cells transfected with full-length or deletion

constructs for myc-tagged AR and flag-tagged TRIM33 (Fig EV4F). Our results show that the AR N-terminal (N) and TRIM33 middle (M) domains are required for mediating the interaction between the two proteins (Fig 5M and N). We explored the functional requirement of the TRIM33 middle domain further by generating a TRIM33 mutant protein without this region (TRIM33- Δ M). As expected, the TRIM33- Δ M protein failed to interact with AR (Fig 5O). More importantly, this mutant protein could not prevent the degradation of AR by Skp2 (Fig 5P) and nor was it recruited to the binding sites of model AR-regulated genes (Fig EV4G).

Next, we asked if the E3 ubiquitin ligase activity of TRIM33 is required for protecting AR from Skp2-mediated degradation. To test this, we overexpressed Skp2 in LNCaP cells along with TRIM33CA, a TRIM33 mutant with point mutations in the RING domain that lacks E3 ubiquitin ligase activity (Dupont *et al.*, 2005). As shown in Fig 5P, wild-type TRIM33, but not TRIM33CA, rescued AR protein level in the presence of Skp2. Together, our results indicate that TRIM33 stabilization of AR from Skp2-mediated degradation requires an intact middle domain and a functional RING domain.

TRIM33 prevents Skp2-mediated ubiquitination of AR

Since our work thus far shows TRIM33 prevents AR from Skp2-mediated degradation, we next determined whether TRIM33 affects the ability of Skp2 to ubiquitinate AR. To test this, we performed a ubiquitination assay on 293T cells overexpressing flag-tagged TRIM33, myc-tagged AR, myc-tagged Skp2, and HA-tagged ubiquitin. As expected, Skp2 overexpression significantly increased AR ubiquitination (Fig 5Q). Moreover, overexpression of wild-type TRIM33, but not TRIM33- Δ M or TRIM33CA, blocked Skp2-mediated ubiquitination of AR (Fig 5Q), suggesting that TRIM33 stabilizes AR through blocking Skp2-mediated ubiquitination of AR.

We also assessed whether androgen-dependent transcription requires TRIM33-mediated stabilization of the AR protein. We tested this by comparing the ability of wild-type TRIM33, TRIM33- Δ M, and

Figure 4. TRIM33 regulates the binding of AR on chromatin.

- A Line plot (upper panel) showing the average AR tag density of the 3,067 AR-TRIM33 shared binding sites in LNCaP cells treated with siTRIM33#1 (left) or siTRIM33#2 (right). Heatmap (lower panel) showing the normalized AR ChIP-seq binding intensities of the same AR-TRIM33 shared binding sites in the upper panel.
- B Genomic snapshots of AR ChIP-seq peaks surrounding FKBP5, KLK3, and KLK2.
- C ChIP-qPCR validation of AR binding sites after TRIM33 knockdown at FKBP5, KLK3, and KLK2 genes in LNCaP and VCaP cells.

Data are represented as a percentage of input chromatin immunoprecipitated. Data are presented as mean \pm SD ($n = 3$ independent experiments); ** $P < 0.01$ (two-way ANOVA).

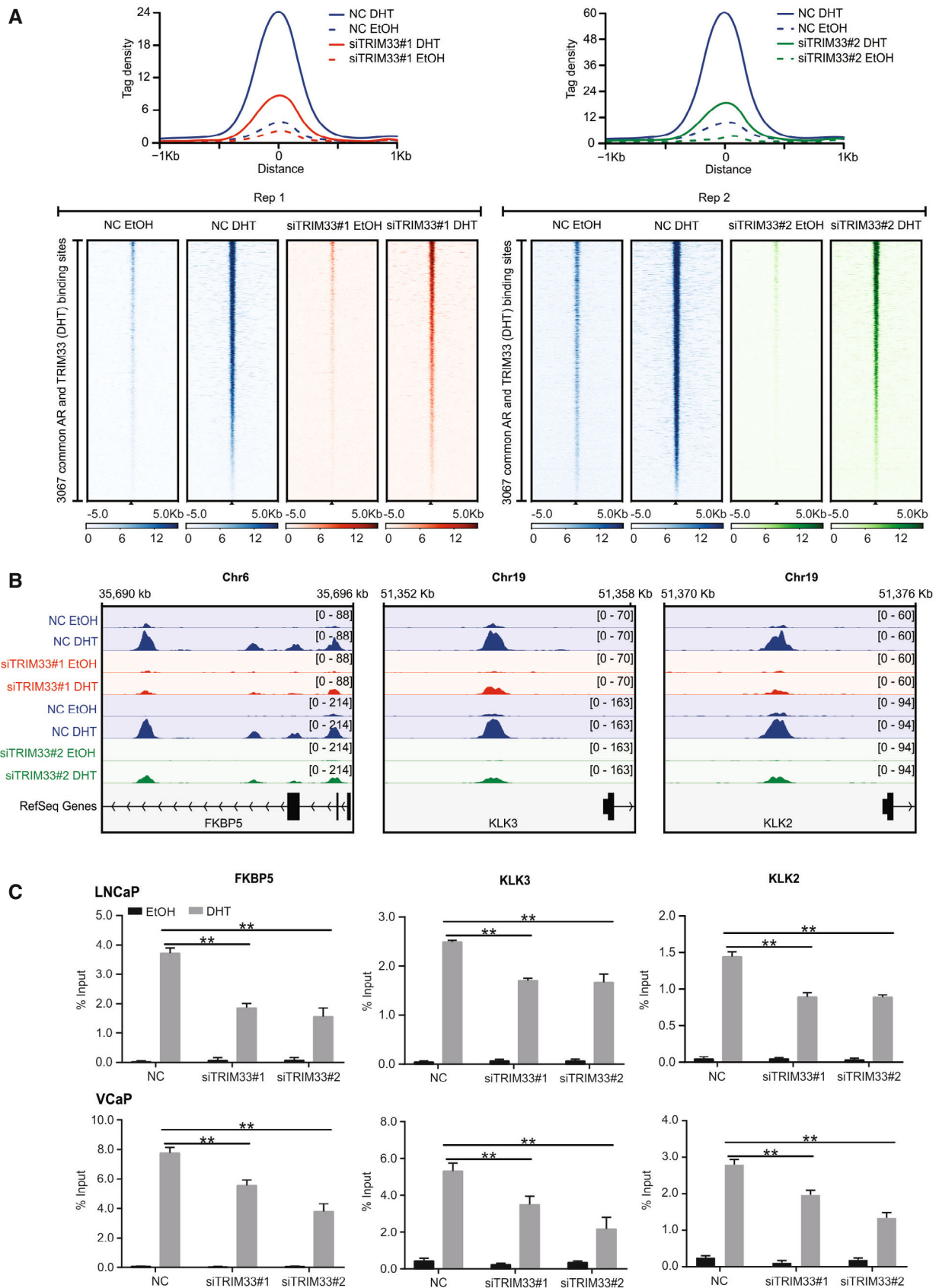


Figure 4.

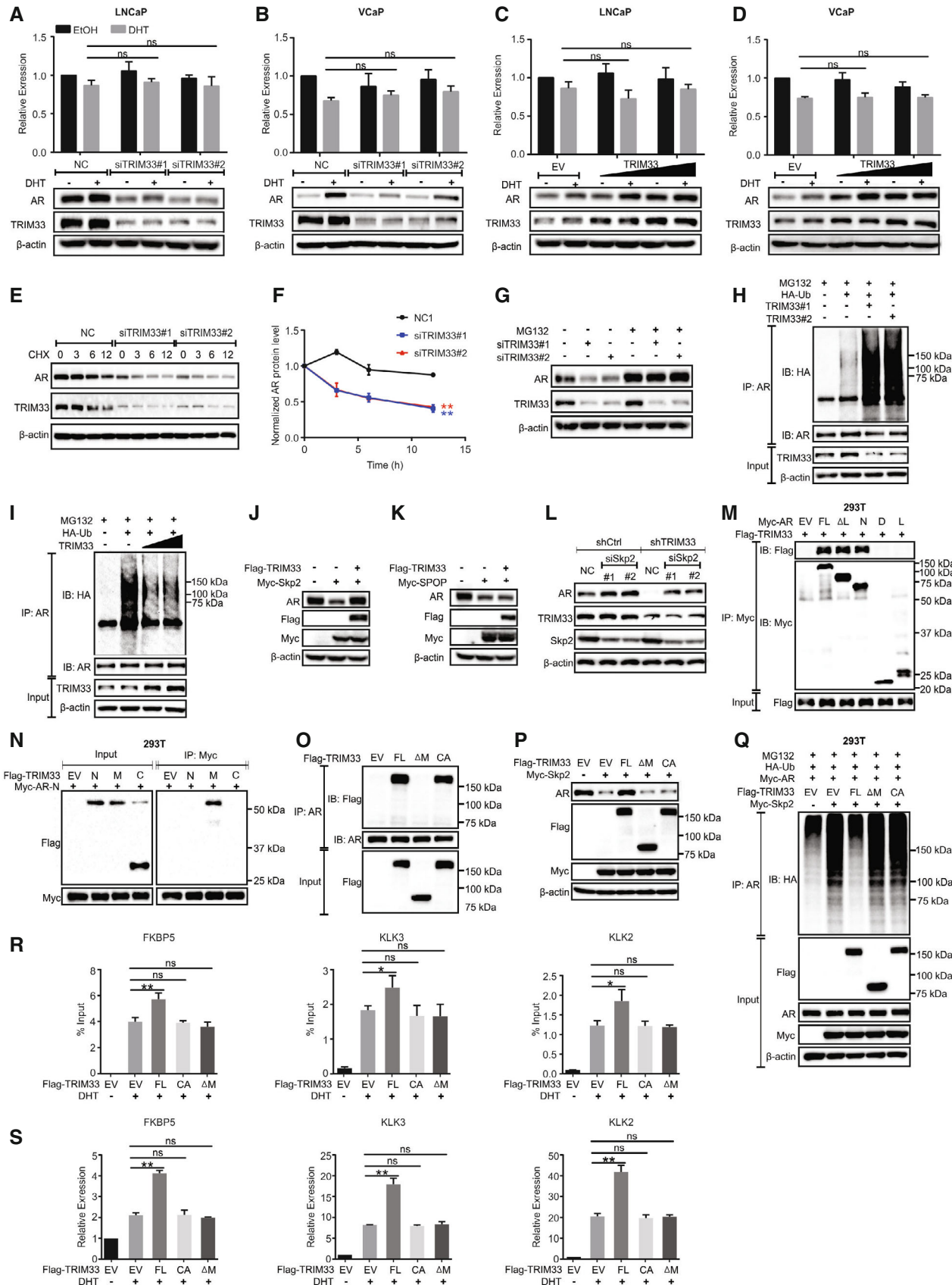


Figure 5.

Figure 5. TRIM33 prevents Skp2-mediated proteasomal degradation of AR.

- A–D AR transcript levels were measured by RT-qPCR on LNCaP cells (A and C) or VCaP cells (B and D) transfected with siTRIM33 or the TRIM33 expression construct and treated with EtOH or DHT. Protein lysates were harvested at 72 h after transfection and subjected to western blot analysis with the indicated antibodies.
- E, F LNCaP cells transfected with siTRIM33 or NC were treated with cycloheximide (CHX). Protein lysates were harvested at the indicated time points for western blot analysis. AR protein levels were quantified and normalized to β -actin and then plotted relative to 0 h.
- G LNCaP cells transfected with siTRIM33 or NC were treated with DMSO or MG132 for 8 h. Protein lysates were extracted and subjected to western blot analysis with the indicated antibodies.
- H, I HA-Ub was expressed in LNCaP cells cotransfected with siTRIM33 (H) or the TRIM33 expression construct (I). The cells were treated with DMSO or MG132 for 4 h before harvesting. Endogenous AR was immunoprecipitated from cell lysates, and interacting proteins were detected by immunoblotting with the indicated antibodies.
- J, K LNCaP cells transiently expressing either myc-tagged Skp2 or myc-tagged SPOP with Flag-TRIM33 were harvested and subject to immunoblot analysis with the indicated antibodies.
- L shTRIM33- or shCtrl-LNCaP cell lines transfected with NC or siSkp2 were harvested 72 h after transfection and subjected to immunoblot analysis with the indicated antibodies.
- M HEK293T cells were cotransfected with flag-TRIM33 and various myc-tagged AR constructs. AR-FL- and AR-truncated mutants were immunoprecipitated with an anti-myc antibody and then subjected to western blot analysis with the indicated antibodies.
- N HEK293T cells were cotransfected with myc-AR-N and various flag-tagged TRIM33 constructs. AR-N was immunoprecipitated with an anti-myc antibody and then subjected to western blot analysis with the indicated antibodies.
- O LNCaP cells were transfected with various flag-tagged TRIM33 constructs. AR-associated proteins were immunoprecipitated with an anti-AR antibody and then subjected to western blot analysis with the indicated antibodies.
- P LNCaP cells were cotransfected with myc-Skp2 and various flag-TRIM33 constructs. AR and other proteins were detected by western blot analysis with the indicated antibodies.
- Q AR pull-down was performed on protein extracts from MG132-treated HEK293T cells overexpressing myc-AR, HA-Ub, myc-Skp2, and various flag-tagged TRIM33 constructs. AR ubiquitination and specific protein levels were detected by western blot analysis with the indicated antibodies.
- R, S LNCaP cells were transfected with various flag-TRIM33 constructs. AR binding was detected by ChIP-qPCR (R), while the expression of AR target genes was detected by RT-qPCR (S).

Data information: In (A–D, F, R, and S), data are presented as mean \pm SD ($n = 3$ independent experiments); * $P < 0.05$, ** $P < 0.01$, ns = not significant (two-way ANOVA). Source data are available online for this figure.

TRIM33CA to regulate chromatin binding and transcriptional activity of AR. Our results show that only wild-type TRIM33 could potentiate AR chromatin binding (Fig 5R) and the transcription of model AR target genes (Fig 5S). Taken together, the above findings suggest that TRIM33 functions as an AR coactivator in PCa by protecting AR from Skp2-mediated ubiquitination and proteasomal degradation.

TRIM33 is overexpressed in human PCa

To examine the clinical significance of TRIM33, we analyzed the expression of TRIM33 in PCa patients (Singh *et al*, 2002; Wallace *et al*, 2008; Taylor *et al*, 2010; Kuner *et al*, 2013; Cancer Genome Atlas Research, 2015; Penney *et al*, 2015; Ding *et al*, 2016; Li *et al*, 2020). Overall, TRIM33 mRNA levels are significantly higher in tumor samples than in normal tissues (Fig 6A). The protein expression of TRIM33 in PCa patient tissues exhibited intense nuclear staining, consistent with its reported nuclear localization (Ferri *et al*, 2015; Xue *et al*, 2015). In addition, the nuclear staining intensity of TRIM33 increased from benign to low Gleason score tumors and further increased in high Gleason score tumors (Fig 6B and C). We also looked at the correlation between AR and TRIM33 expression in PCa patients. From our analysis of the TCGA PCa dataset, we found a positive correlation between TRIM33 mRNA and AR protein levels (Fig EV5). Together, these clinical data suggest a pro-tumorigenesis function of TRIM33 by stabilizing AR protein levels in PCa.

An AR-TRIM33 coregulated gene signature is highly expressed in PCa and predicts disease recurrence

To further evaluate the clinical significance of TRIM33 coregulation of the AR transcription program in PCa, we associated the AR and

TRIM33 cistromes with transcriptome data from LNCaP cells and defined an AR-TRIM33-coactivated gene signature consisting of 36 genes. This gene signature is positively correlated with previously published AR-regulated gene signatures derived from PCa patients (Nelson *et al*, 2002; Hieronymus *et al*, 2006) across multiple PCa cohorts (Singh *et al*, 2002; Wallace *et al*, 2008; Taylor *et al*, 2010; Kuner *et al*, 2013; Cancer Genome Atlas Research, 2015; Penney *et al*, 2015; Ding *et al*, 2016; Li *et al*, 2020), suggesting our gene signature is regulated by AR in PCa tumors (Fig 7A). The average expression of our gene signature is also, in general, significantly higher in tumor samples compared with normal tissues in the same studies (Fig 7B). Moreover, we were able to stratify PCa patients into two clusters based on whether they have “high” (orange) or “low” (blue) expression of our gene signature (Fig 7C and D). Notably, patients in the “high” cluster showed a significantly higher chance of disease recurrence (Fig 7E). Together, our clinical analyses highlight an oncogenic role for TRIM33 in PCa and provide a gene signature with predictive value.

TRIM33 is required for prostate tumor growth

The above clinical findings and our functional enrichment analyses (Fig 3H) of the AR-TRIM33 coregulated transcriptome indicate that TRIM33 might coordinate with AR to promote PCa growth and survival. To test this possibility, we examined the effect of TRIM33 depletion on PCa cell growth. Our results show that TRIM33 knock-down significantly reduced cell growth in LNCaP and VCaP cells (Fig 8A and B). We explored the cause behind the reduction in cell growth by examining whether TRIM33 has a role in the cell cycle and apoptosis. In FACS analyses, the depletion of TRIM33 shifted cells to the G1 phase of the cell cycle (Fig 8C and D) and increased the number of apoptotic cells (Fig 8E and F). Together, these results

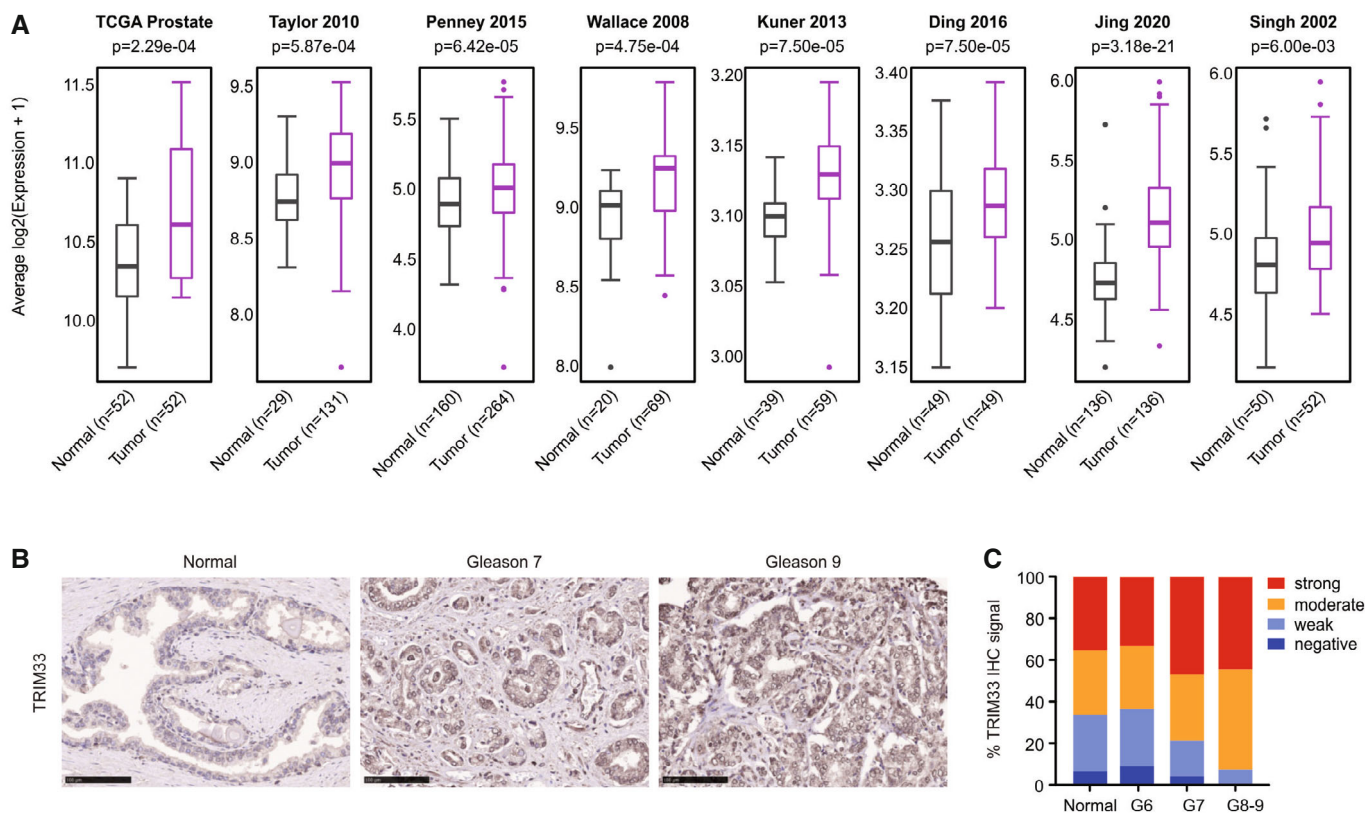


Figure 6. TRIM33 is overexpressed in PCA.

A TRIM33 mRNA expression levels were analyzed in normal and tumor samples from multiple publicly available patient cohorts. A two-sided Wilcoxon signed-rank test was used for the TCGA Prostate, Ding *et al* (2016), and Li *et al* (2020) datasets, while a two-sided Wilcoxon rank-sum test was used for the other datasets. Measurements shown in box plots are the first and third quartiles and are split by the medians, whiskers extending a 1.5-fold interquartile range beyond the box.

B, C A human PCA progression tissue microarray was used for immunohistochemistry staining. Representative staining images are shown in (B). TRIM33 staining by Gleason Scores is summarized in the histogram. Scale bar: 100 μ m.

suggest that TRIM33 promotes cell proliferation by arresting the cell cycle and inhibiting apoptosis.

To examine the tumorigenic role of TRIM33 *in vivo*, we established stable TRIM33 knockdown (shTRIM33) and control (shCtrl) LNCaP cell lines (Appendix Fig S2A and B). Similar to our *in vitro* transient studies, shTRIM33 stable cells displayed a lower proliferation rate than control cells (Appendix Fig S2C). We analyzed the *in vivo* role of TRIM33 by injecting the stable cell lines into male nude mice and monitored their growth. shTRIM33 stable cells showed statistically significant retarded tumor growth compared shCtrl cells (Fig 8G and H). shTRIM33 tumors also exhibited significantly reduced weight (Fig 8I). Western blot analysis confirmed that AR protein levels are lower in shTRIM33 tumors than shCtrl tumors (Fig 8J). Taken together, our *in vivo* results reveal a tumorigenic role for TRIM33 in PCA.

TRIM33 sensitizes PCa cells to the anti-proliferative effects of AR antagonists

Elevated AR protein stability is one of the underlying mechanisms of antiandrogen therapy resistance (Gregory *et al*, 2001; Chen *et al*, 2004). Given that our work shows TRIM33 stabilizes AR from

Skp2-mediated ubiquitination and degradation, we tested whether reducing TRIM33 levels sensitizes PCa cells to clinically approved AR antagonists, Bicalutamide (Casodex) and Enzalutamide (MDV3100). A dose-response of the two drugs on shTRIM33 and shCtrl-LNCaP cells shows that a combination of TRIM33 suppression and antagonist treatment resulted in a more potent anti-proliferative effect on PCa cells compared with only AR antagonist treatment (Appendix Fig S3A and B). Moreover, depletion of TRIM33 significantly lowered the half-maximal inhibitory concentration (IC₅₀) of Casodex and MDV3100 (Fig 8K). Together, these findings suggest that TRIM33 sensitizes PCa cells to Casodex and MDV3100 and could be a promising therapeutic target for PCa treatment.

Discussion

Androgen receptor-mediated transcriptional regulation remains a primary driver throughout the different stages of PCa development (Feldman & Feldman, 2001; Heemers & Tindall, 2009; Massie *et al*, 2011; Decker *et al*, 2012; Grasso *et al*, 2015). Coregulatory proteins work in conjunction with each other to tightly control the

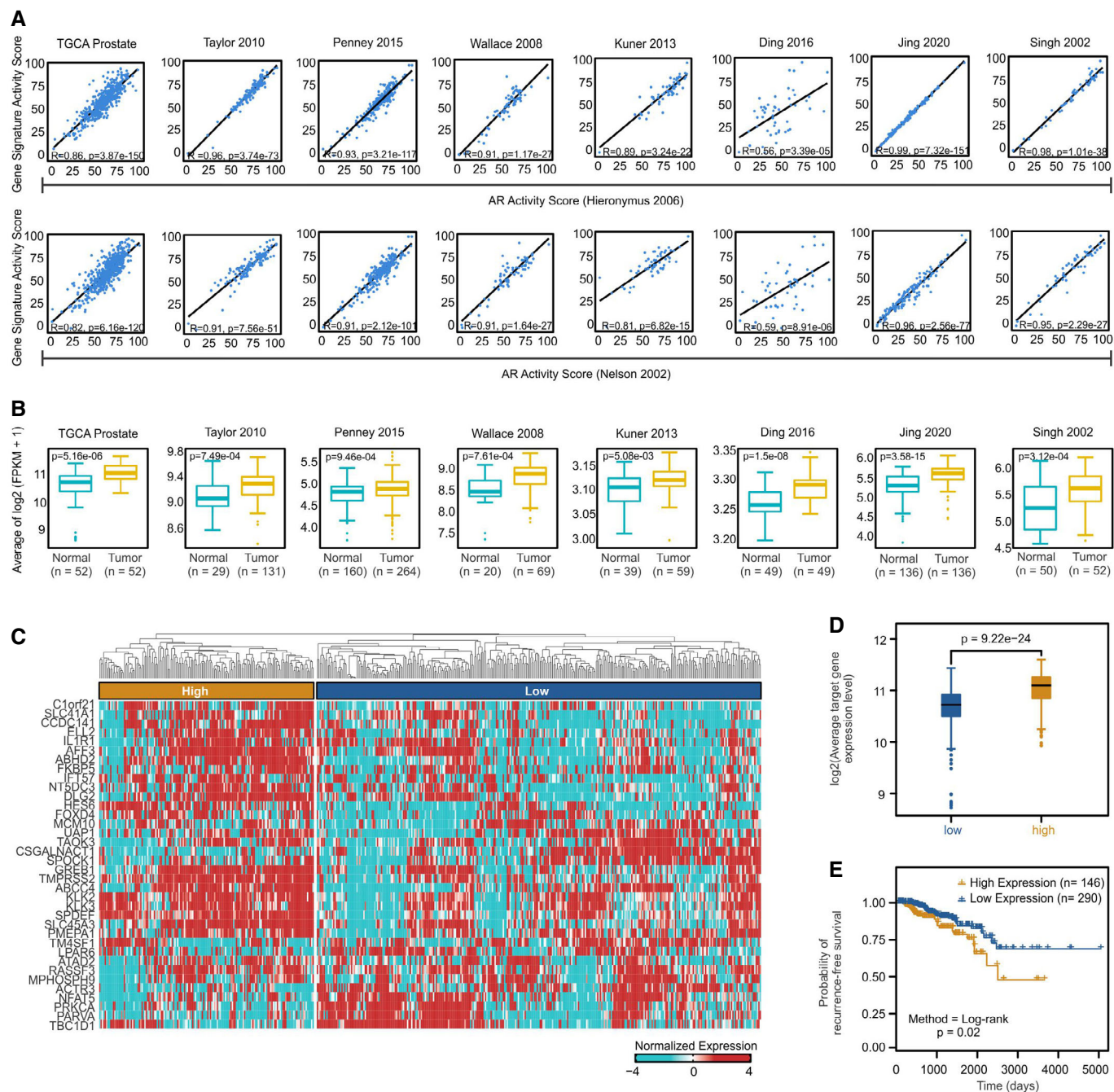


Figure 7. AR-TRIM33 coregulated target genes define a signature that is highly expressed in PCa tumors and predicts disease recurrence.

- A The AR-TRIM33-coactivated gene signature was compared with two PCa patient-derived AR gene signatures in multiple publicly available patient datasets.
- B The expression of the gene signature in normal and tumor samples was examined in the same cohorts used in (A). A two-sided Wilcoxon signed-rank test was used for the TCGA Prostate, Ding *et al* (2016), and Li *et al* (2020) datasets, while a two-sided Wilcoxon rank-sum test was used for the other datasets. Measurements shown in box plots are the first and third quartiles and are split by the medians, whiskers extending 1.5-fold interquartile range beyond the box.
- C Hierarchical clustering of PCa patients from the TCGA Prostate dataset ($n = 480$) resulted in two distinct clusters indicated in orange (high) and blue (low) based on the average expression of our 36-gene signature.
- D Boxplot showing the average expression level of the 36 AR-TRIM33-coactivated genes for the low and high clusters in (D). Measurements shown in box plots are the first and third quartiles and are split by the medians, whiskers extending 1.5-fold interquartile range beyond the box. Statistical analysis was performed using the Wilcoxon rank-sum test.
- E Kaplan–Meier analysis showing the recurrence-free survival of patients with low and high expression of the 36-gene signature (P -value, log-rank test).

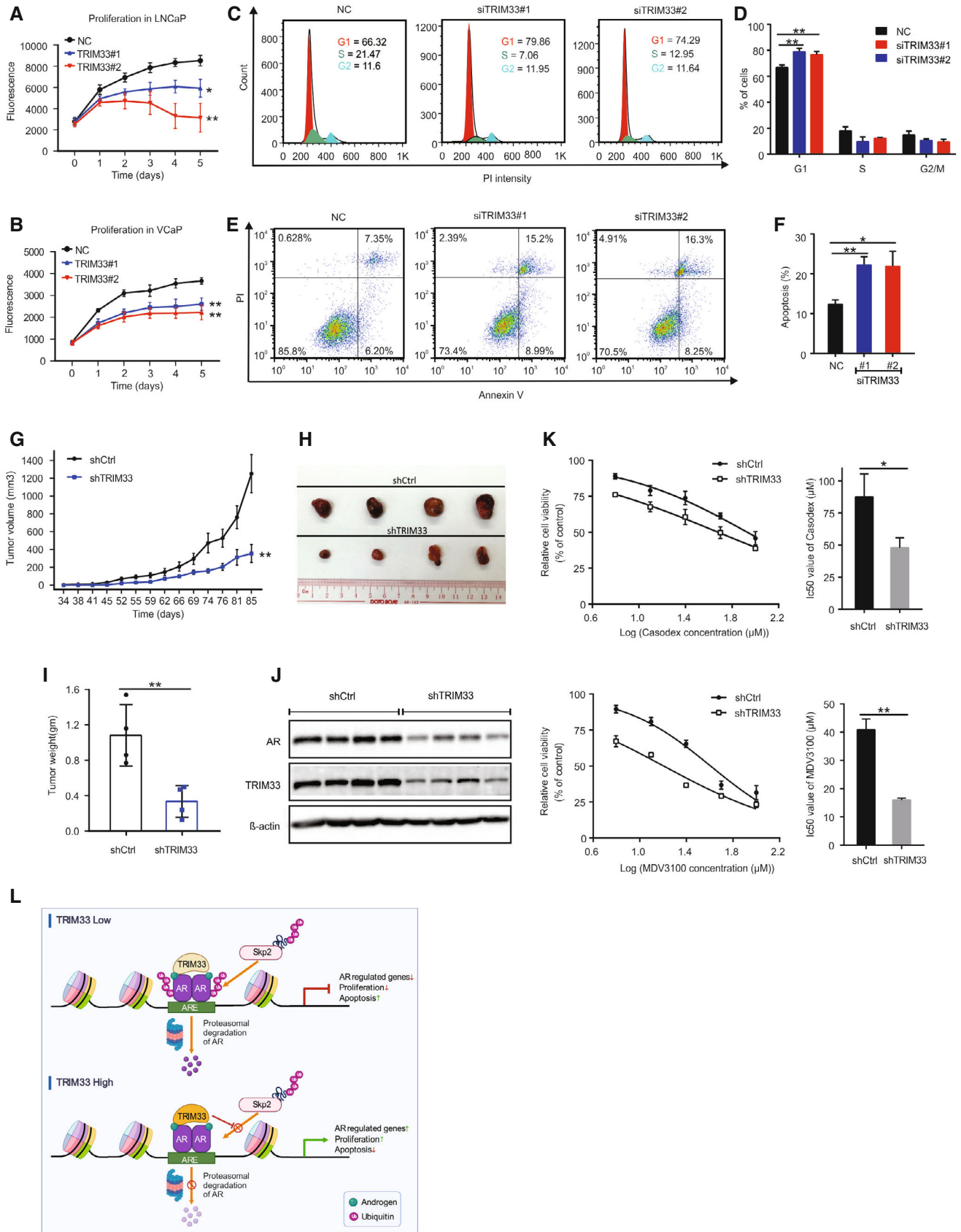


Figure 8.

Figure 8. TRIM33 is required for prostate tumor cell growth *in vitro* and *in vivo*.

- A, B AlamarBlue assays were performed on LNCaP cells (A) and VCaP cells (B) treated with siTRIM33 or NC at the indicated times ($n = 3$ independent experiments).
- C–F Flow cytometry analyses were performed on LNCaP cells transfected with siTRIM33 or NC for detecting cell cycle (C) and cell apoptosis (E). The bar charts show the distribution of cells in each cell cycle phase from C (D) or the percentage of apoptotic cells from E (F) under indicated conditions ($n = 3$ independent experiments).
- G–I TRIM33 depletion reduced prostate xenograft tumor growth. LNCaP cells stably expressing shCtrl or shTRIM33 were inoculated in the right flanks of male nude mice. Tumor growth was measured twice per week, as shown in (G). Tumors were excised at the endpoint (H) and weighed (I) ($n = 4$ mice/group).
- J Western blot analysis of AR and TRIM33 protein levels in tumor tissues from (H).
- K AlamarBlue assay was used to measure the viability of shTRIM33- or shCtrl-LNCaP cell lines with 72 h of treatment of different amounts of Casodex (upper panel) or MDV3100 (lower panel). Cell viability values of cells under specific conditions were normalized to the cell viability values of untreated cells. Cytotoxicity plots (left panels) represent $n = 3$ independent experiments with six replicates per drug concentration for each experiment. Bar graphs (right panels) show the IC_{50} value.
- L A model depicting the role of TRIM33 on AR signaling in PCa. TRIM33 is relatively lowly expressed in normal conditions, allowing Skp2 to ubiquitinate and degrade AR. In PCa where TRIM33 is highly expressed, TRIM33 binds to AR and prevents AR from Skp2-mediated ubiquitination and subsequent proteasomal degradation, thereby enhancing AR signaling and driving PC tumor growth. The model was created with BioRender.com.
- Data information: In (A, B, E, F, G, I, and K), data represent the mean \pm SD; * $P < 0.05$; ** $P < 0.01$ (two-way ANOVA).

transcriptional activity of AR (Heinlein & Chang, 2002). Alterations in the expression or activity of these coregulators will lead to an AR transcriptional landscape that promotes PCa progression, highlighting the critical function and therapeutic value of coregulators in PCa (Wang *et al*, 2009; Sharma *et al*, 2013; Mills, 2014; Pomerantz *et al*, 2015). Here, we used a highly robust proteomics approach to discover all chromatin-bound AR-interacting proteins in PCa cells. We also identified and functionally characterized TRIM33 as a novel coregulator of AR and mediator of PCa carcinogenesis (Fig 8L).

Thus far, previous studies on TRIM33 have implicated it as a tumor suppressor with transcriptional corepressor activity (Dupont *et al*, 2005, 2009; He *et al*, 2006; Vincent *et al*, 2009; Agricola *et al*, 2011; Aucagne *et al*, 2011; Herquel *et al*, 2011; Kulkarni *et al*, 2013; Ferri *et al*, 2015; Xue *et al*, 2015). In contrast, our study in PCa demonstrates that TRIM33 can also act as an oncogene, indicating that TRIM33 functions in a context-dependent manner. Specifically, we show that TRIM33 acts as a transcriptional coactivator of pro-mitotic genes, and the loss of TRIM33 significantly slows down prostate tumor growth. In support of this finding, both TRIM33 mRNA and protein levels are significantly elevated in human PCa tumor specimens compared with normal tissues. Our work also revealed that TRIM33 is an integral component of the AR transcriptional network, with alterations in TRIM33 levels resulting in a profound impact on the global AR transcriptome. Overall, our findings support TRIM33 as a coactivator of AR in PCa. We show that the activation of AR upregulated genes is dependent on TRIM33, and this regulation is due to the direct coordinated actions of TRIM33 on AR chromatin binding, especially at the enhancer regions of genes associated with PCa development. Moreover, we discovered TRIM33-regulated AR target genes define an AR-TRIM33-coactivated gene signature, which is highly expressed in PCa tumors, and patients with high expression of this gene signature show a higher risk of disease recurrence. While our current work implicates the importance of TRIM33 on AR-regulated transcription in PCa, additional detailed dose–response experiments will be needed in the future to determine the exact contribution of TRIM33 on AR protein level and transcriptional activity.

The ubiquitin-mediated proteasome degradation pathway is one of the primary mechanisms for modulating protein turnover, and dysregulation of this process has been implicated in the development and progression of many diseases, including cancer (Hoeller *et al*, 2006; Morrow *et al*, 2015; Mansour, 2018). In this work, we show that TRIM33 stabilizes AR protein levels in PCa cells by

preventing ubiquitin-mediated proteasomal degradation of AR. Notably, we find TRIM33 preferentially inhibits Skp2- but not SPOP-mediated AR degradation, suggesting precise control of AR protein levels through specific pairs of degrader-protector proteins. How does TRIM33 abolish Skp2-mediated ubiquitination and degradation of AR? Our findings show that this process requires the direct physical interaction between TRIM33 and AR. Our preliminary studies also suggest that TRIM33 does not disrupt the interaction between AR and Skp2 (unpublished observation). However, we know the RING domain of TRIM33 is required to prevent AR from Skp2-mediated ubiquitination and degradation, indicating the necessity of the E3 ligase activity of TRIM33. Thus, we speculate that TRIM33 may impede AR degradation by inhibiting Skp2 E3 ligase activity or promoting the degradation of Skp2. It is also possible that TRIM33 may promote the function or recruitment of other coregulators through its E3 ligase activity, which then subsequently interferes or blocks Skp2-mediated ubiquitination of AR. These and other possibilities will be tested in future work.

Current PCa therapies mainly target the androgen-dependent activation of AR. However, patients frequently become resistant to these therapies via multiple mechanisms, including increased AR protein stability (Gregory *et al*, 2001; Chen *et al*, 2004). Our studies show that TRIM33 stabilizes AR from Skp2-mediated ubiquitination and degradation, which raises the possibility that inhibiting TRIM33 could potentially enhance the efficacy of clinically approved AR antagonists. Indeed, our findings suggest that combining small molecules targeting TRIM33, which would lower AR protein levels, together with AR antagonists, could be used to achieve synergistic effects in PCa treatment, including advanced stages of the disease. Moreover, another mechanism underlying therapy resistance is the expression of AR variants, such as AR-V7 (Hu *et al*, 2009). We find that TRIM33 can also interact with AR-V7 and regulate AR-V7 protein expression similarly. Together, our work suggests TRIM33 is a potential therapeutic target for both primary and therapy-resistant PCa.

TRIM33 is closely related to TRIM24 and TRIM28, and these three proteins belong to a subfamily of TRIMs (Hatakeyama, 2017). TRIM24 and TRIM28 are also strong AR interactors from our RIME assay (Dataset EV1) and were recently reported to function in AR-dependent transcription in PCa (Kikuchi *et al*, 2009; Groner *et al*, 2016). Our preliminary studies indicate that TRIM24, TRIM28, and TRIM33 are co-occupied with the enhancers of model AR target genes (unpublished observations). Furthermore, we found TRIM24

depletion inhibited while TRIM28 depletion activated AR-regulated genes (unpublished observations). Together, these findings raise the possibility that TRIM24, TRIM28, and TRIM33 might operate as a trimeric complex to regulate AR transcriptional activity. In supporting this possibility, these three TRIMs physically and functionally interact together to modulate hepatocellular carcinoma (HCC) formation in mice (Herquel *et al*, 2011). Whether this cooperation also occurs in PCa will require further investigation.

In summary, we describe a noncanonical role for TRIM33, serving as a coactivator of AR-dependent transcription in PCa. Our work also provides detailed mechanistic insights on how AR coordinate with coregulators in promoting PCa progression. More importantly, the regulation of AR transcriptional activity by TRIM33 provides a potentially important pathway that can be targeted for PCa therapy.

Material and Methods

Chemicals

Dihydrotestosterone (DHT) was purchased from Tokyo Chemical Industry. Cycloheximide (CHX) was purchased from Sigma Aldrich. MG132 was purchased from Selleck Chemicals. Bicalutamide (Casodex) and Enzalutamide (MDV3100) were purchased from Adooq Bioscience. The following antibodies were used for RIME, ChIP, IHC, and western blot assays: anti-AR (H280 and N-20), rabbit IgG, and anti-c-Myc (9E10) from Santa Cruz, anti-HA (6E2) from CST, anti-TRIM33 (A301-059A and A301-060A) from Bethyl Laboratories, anti- β -actin (AC-15) and anti-FLAG from Sigma.

Cell culture

LNCaP and VCaP cells were purchased from ATCC, maintained in RPMI (Gibco) and DMEM (Gibco), respectively, and supplemented with 10% FBS (Gibco). Cells with passage < 30 were used for all experiments. Before hormone treatment, LNCaP cells were maintained in a hormone-depleted condition in phenol red-free RPMI supplemented with 5% charcoal-dextran-treated FBS (CDFBS; Hyclone) for a minimum of 72 h. Similarly, VCaP cells were maintained in phenol red-free DMEM supplemented with 10% CDFBS for a minimum of 72 h. Additionally, cells were regularly tested for mycoplasma contamination using the MycoAlert mycoplasma detection kit (Lonza).

Plasmids and reporter assay

Full-length flag-tagged TRIM33 pCS2-FLAG-TRIM33 and the TRIM33 mutant pCS2-FLAG-TRIM33CAmut plasmids were purchased from Addgene. The pCS2-FLAG-TRIM33- Δ M (deletion of 446–888aa) construct was generated by PCR using the pCS2-FLAG-TRIM33 plasmid as a template. FLAG-TRIM33-N (which includes the RING finger, 2 B-boxes, and a CC domain, 36–445aa), -M (446–888aa), and -C (which includes the PHD/bromodomain, 889–1,127aa) were subcloned into the p3 \times FLAG-CMV26 vector (a generous gift from Dr. Gang Li (University of Macau)). Myc-AR full length (FL), N (NTD, 1–559aa), D (DBD and hinge region, 555–672 bp), L (LBD, 673–920aa), and Δ L (1–672aa) were subcloned into the pcDNA6-myc/His A vector (a generous gift from Dr. Chuxia Deng (University of

Macau)). The pRK5-HA-Ubiquitin plasmid was a generous gift from Dr. Gang Li (University of Macau). The AR reporter plasmid used in this study has been described previously (Tan *et al*, 2012). The pcDNA3-myc-Skp2 plasmid was a generous gift from Dr. Zhenbang Chen (Meharry Medical College). The myc-SPOP plasmid was a generous gift from Dr. Jindan Yu (Ohio State University). For ectopic expression, LNCaP cells were transfected with the indicated plasmids using Lipofectamine 3000 (Invitrogen) according to the manufacturer's protocol. For the AR reporter assay, pGL4-ARE-TATA-LUC and Renilla plasmids were cotransfected with pCS2-FLAG-TRIM33 using Lipofectamine 3,000 or siTRIM33 and/or siAR using Lipofectamine RNAiMAX (Invitrogen) in LNCaP cells. Following transfection, the culture media was changed to phenol-free RPMI. 48 h post-transfection, cells were treated with 10 nM of DHT or EtOH for another 24 h before quantifying the luciferase activity using the Dual-Glo luciferase kit (Promega).

RNAi studies

LNCaP or VCaP cells cultured for 24 h in phenol red-free medium were transfected with 5 nM Dicer-substrate short interfering RNAs (DsiRNAs) from IDT using Lipofectamine RNAiMAX according to the manufacturer's protocol. Forty-eight hours after transfection, cells were treated with EtOH or 10 nM DHT for the specified time before harvesting for RT-qPCR, RNA-seq, and western blot analyses. For every target, two separate DsiRNAs were paired with the negative control nontargeting DsiRNA (NC). DsiRNA and real-time qPCR primer sequences are listed in Table EV2 in the supplemental material section. Gene expression profiles for knockdown studies were obtained from at least three independent experiments.

Cell proliferation assay

LNCaP cells were transfected with siTRIM33 or NC in 6-well cell culture plates. After 24 h of transfection, the cells were trypsinized, and 20,000 cells were seeded into each well of a 96-well cell culture plate. Cell proliferation was quantified using the alamarBlue cell viability reagent (Invitrogen) for 5 consecutive days at 24 h intervals according to the manufacturer's protocol.

Flow cytometry

LNCaP cells were seeded at 1.0×10^6 cells/well in 6-well cell culture plates and maintained in RPMI 1640 supplemented with 10% FBS. The following day, cells were transfected with 5 nM of siTRIM33 or NC using Lipofectamine RNAiMAX according to the manufacturer's protocol. Seventy-two hours after transfection, cells were stained with Propidium Iodide (Sigma) for cell cycle detection or Alexa Fluor™ 488 Annexin V/Dead Cell Apoptosis Kit (Invitrogen) for cell apoptosis analysis. Cell cycle and apoptosis data were acquired using the BD FACSCalibur and analyzed with the FlowJo software.

Chromatin immunoprecipitation (ChIP) and ChIP-seq

ChIP assays were performed as previously described (Holmes *et al*, 2016). Briefly, for TRIM33 ChIP, approximately 1×10^7 LNCaP cells cultured in hormone-starved conditions for 72 h were

treated with 100 nM DHT or EtOH for 2 h. Similarly, for AR ChIP in TRIM33 knockdown cells, approximately 5×10^6 cells were transfected twice with 5 nM of siTRIM33 as described above, followed by 100 nM DHT or EtOH treatment for 2 h. Cells were then cross-linked with 1% formaldehyde (Sigma), followed by immunoprecipitation with the specific antibody-coated protein G Dynabeads (Invitrogen). The precipitated DNA was de-cross-linked at 65°C for 8–18 h and subjected to either high-throughput sequencing or RT-qPCR at specific genomic regions.

RIME

AR-RIME was performed as described (Mohammed *et al.*, 2016). Briefly, approximately 2×10^7 cells cultured in hormone-starved conditions for 72 h were treated with 100 nM DHT for 2 h. The cells were then cross-linked with 1% methanol-free formaldehyde (Thermo Scientific) for 8 min at RT. Immunoprecipitation was carried out using 100 μ l protein G Dynabeads (Invitrogen) coated with 10 μ g anti-AR or rabbit IgG antibody. The bound proteins were extracted by heating in 20 μ l of denaturing buffer (0.02 M Tris-HCl, pH 6.9, 2% SDS, 0.1 M dithiothreitol) for 10 min. After spinning at $14,000 \times g$ for 30 s, the supernatant containing the extracted proteins was collected and stored at -80°C before proteomic analysis.

Label-free LC-MS/MS quantitative proteomic analysis

The extracted proteins were subjected to trypsin digestion using the filter-aided sample preparation approach described previously (Wisniewski, 2018). The tryptic digest was cleaned up with a C18 ZipTip (Millipore) according to the manufacturer's instructions. After drying down with a SpeedVac, the cleaned peptides were reconstituted in 5% acetonitrile (ACN) and water 95% with 0.1% formic acid. Peptides were separated on an EASY-Spray™ LC column 75 $\mu\text{m} \times 50$ cm, 2- μm 100-Å pore size (Thermo Scientific) with an ACN gradient from 5 to 35% in 0.1% formic acid over 65 min. Peptides eluting from the column were analyzed on a Q Exactive mass spectrometer (Thermo Fisher Scientific) operated in a data-dependent mode. Survey full-scan MS spectra (400–2,500 m/z) were acquired at 70,000 FWHM resolution. The top 20 most intense ions were sequentially isolated and fragmented in the orbitrap by higher-energy collisional dissociation (HCD) with normalized collision energy (NCE) set to 25. MS/MS spectra were acquired at 17,500 FWHM resolution. The LC-MS/MS data were searched against the UniProt human protein sequence (reviewed) database using MaxQuant v1.5.3.17 (Cox & Mann, 2008) to identify proteins with a minimum of two unique peptides at PSM FDR of 0.01, dependent peptide FDR of 0.01, and protein FDR of 0.01. For label-free quantification, the LFQ intensity of each unique protein was calculated using the intensity data of the unmodified unique peptides and razor peptides.

ChIP-seq analysis

We performed single- and paired-end Illumina sequencing for ChIP-seq. For paired-end sequencing, only R1 reads were used for analyses. All ChIP-Seq reads were mapped on the human genome assembly version hg19 using Bowtie v.0.12.9 (Langmead *et al.*, 2009) with default parameters. Potential PCR artifacts and read duplications from alignments (BAM files) were marked using Picard

MarkDuplicates v.2.20 (<https://broadinstitute.github.io/picard/>) and then processed with MACS v.1.4.2 (Zhang *et al.*, 2008) for peak calling (P -value $\leq 1e-04$). The peak overlap between AR and TRIM33 cisomes was calculated using the findOverlapsOfPeaks function from the ChIPpeakAnno v.3.16.1 R package (Zhu *et al.*, 2010). ChIPseeker v.1.18 was used to annotate ChIP-seq peaks (Yu *et al.*, 2015). The deepTools v.3.2.1 (Ramirez *et al.*, 2016) package was used to generate tag density heatmaps around the ChIP-seq peak center (± 5 Kb). To determine the effect of TRIM33 knockdown on AR binding, we sub-sampled an equal number of aligned reads for all the samples to compensate for sequencing bias. The standalone version of the Integrative Genomics Viewer (IGV v.2.5.2) was used for peak visualization of selected genes (Thorvaldsdottir *et al.*, 2013). HOMER v4.11.1 was used for motif enrichment analysis (Heinz *et al.*, 2010).

RNA-seq analysis

The total RNA of each sample was extracted using the RNeasy Mini Kit (QIAGEN). Next-generation sequencing libraries were constructed using the NEBNext® Ultra™ Directional RNA Library Prep Kit for Illumina® according to the manufacturer's protocol. Sequencing was performed using 2×100 bp paired-end (PE) on the HiSeq 2000 System with an average read length of around 85 base pairs. The raw reads of every sample were first trimmed to 75 bp and then mapped as paired-end sequencing reads against the UCSC hg19 genome and the gene annotation reference GRCh37 using HISAT2 (Kim *et al.*, 2015). The FPKM (Fragments Per Kilobase of exon model per Million mapped fragments) expression values were calculated from the BAM file generated by HISAT2 and SAMtools (Li *et al.*, 2009) using the StringTie package (Pertea *et al.*, 2015). Genes with FPKM greater than zero in all samples and median FPKM across all samples equal or greater than one was retained for further analysis. The sequencing quality was evaluated using the FastQC and RSeQC packages (Wang *et al.*, 2012). GSEA was performed using the standalone version of GSEA v4.1.0. Functional enrichment analysis was performed using the DAVID v6.8 database (Huang *et al.*, 2007). Heatmaps of differentially expressed genes were created with the R package pheatmap.

Clinical samples, tissue microarray assay (TMA), and immunohistochemistry (IHC) analysis

For IHC analysis, 114 formalin-fixed paraffin-embedded prostate tissue specimens from radical prostatectomy were selected from the Department of Pathology, Queen Mary Hospital, The University of Hong Kong. Ethics approval for the study was obtained at the Institutional Review Board of the University of Hong Kong/Hospital Authority Hong Kong West Cluster. The archival dates of the specimens were between 2005 and 2011. The age of patients at the time of tissue procurement ranged from 48 to 76 years old (median age of 67 years). Median follow-up 119 months (ranging from 33 to 170 months). Sixty-seven patients (61.4%) had preoperative prostate-specific antigen (PSA) level less than 10 ng/ml. The tissue panel included 114 prostatic acinar adenocarcinomas and adjacent paired normal prostate tissue. Tissue samples with prior hormonal or radiation therapy treatment were excluded. Histological diagnoses were reviewed and graded by pathologist Tang AHN using the

updated Gleason grading system (2014 update; Epstein *et al*, 2016a) and the WHO/ISUP Grade group (Epstein *et al*, 2016b). The distribution of Gleason score and grade group, and patients' clinical information are summarized in Table EV3.

All 114 prostate specimens were used to construct four tissue microarrays (TMA). Representative areas (carcinoma and normal tissue) of each specimen were marked. The carcinoma component was sampled in triplicates to account for tumor heterogeneity. A haematoxylin and eosin (H&E) stained section from each TMA block was assessed by Tang AHN to ensure targeted tissues had been accurately sampled.

For TRIM33 immunohistochemical staining, 4 μ m paraffin sections from TMAs were obtained. They were deparaffinized in xylene and rehydrated in graded alcohol and distilled water. Heat-induced antigen retrieval was performed in Tris-EDTA buffer solution (pH 8.0). The sections were incubated with anti-TRIM33 overnight at 4°C. UltraVision Quanto Detection System HRP (Thermo Scientific) was used for visualization according to the manufacturer's protocol. Staining was revealed by counter-staining with haematoxylin. Staining intensity was graded on a 0–3 scale (0: Negative, 1: weak, 2: moderate, 3: strong).

Gene signature and survival analysis

The AR-TRIM33 coregulatory gene signature ($n = 36$) was defined by genes associated with AR-TRIM33 cobinding within $-/+75$ Kb of the TSS and downregulated by TRIM33 knockdown in both RNA-seq replicates (androgen Foldchange ≥ 2 and siTRIM33 Foldchange ≤ -1.2). The expression of the AR-TRIM33-coactivated gene signature was used to stratify patients in the TCGA PCa clinical cohort ($n = 482$) into high and low expression groups using hierarchical clustering on the scaled expression (z -score) of the AR-TRIM33-coactivated gene signature. ComplexHeatmap v2.1.0 was used to plot the heatmap (Gu *et al*, 2016). The average gene expression of the AR-TRIM33-coactivated gene signature was compared to assess the difference between stratified groups, and the significance was calculated using a two-sided Wilcoxon rank-sum test ($P < 0.001$). The probability of recurrence-free survival was calculated based on the stratified group information. The Survival v3.1.8 R package was used to perform the statistical analysis, and the Surminer v0.4.6 R package was used to draw the Kaplan–Meier plot.

Correlation analysis

The interplay between AR- and TRIM33-regulated genes in clinical samples were analyzed using our defined gene signature ($n = 36$) and two previously published AR gene signatures (Nelson *et al*, 2002; Hieronymus *et al*, 2006). We calculated the activity score for each of the signatures separately using the method described previously (He *et al*, 2018). Briefly, log₂ transformed gene expression values were converted to z -scores for each sample and then consolidated for all the genes. The consolidated z -score was then normalized using percentile min-max normalization, which then named the activity score for each gene signature into values ranging from 0 (Minimum activity score) to 100 (Maximum activity score). Finally, the correlation between our gene signature and the AR activity score for each specimen was calculated using the Pearson correlation coefficient method. The results were plotted

using the ggscatter function implemented in ggpubr v0.2.4 with R and P -values ($P < 0.001$).

Coimmunoprecipitation (Co-IP)

Co-IP assays were performed as previously described (Paltoglou *et al*, 2017). In brief, 8.0×10^6 LNCaP or 1.0×10^7 VCaP cells were seeded in 15 cm dishes and grown in hormone-deprived media for 72 h. Nuclear lysates were extracted according to the RIME protocol and immunoprecipitated overnight with 100 μ l protein G Dynabeads (Invitrogen) coated with 5 μ g anti-AR antibody or rabbit IgG. Beads were washed three times with PBS, boiled in $2 \times$ SDS-PAGE sample buffer at 95°C for 5 min, and analyzed by western blotting.

GST pull-down assay

GST and his-MBP recombinant proteins were expressed in BL21 Rosetta (DE3) cells (Novagen). GST proteins were purified using Glutathione Sepharose 4B beads (GE Healthcare) according to the manufacturer's protocol. His-MBP proteins were purified using HisPur™ Ni-NTA Superflow Agarose (Thermo Scientific) according to the manufacturer's protocol. GST proteins immobilized on Glutathione Sepharose 4B beads were mixed with his-MBP proteins on a rotator at 4°C for 4 h. The beads were then washed three times, eluted with 30 μ l of $1 \times$ SDS-PAGE loading buffer, boiled at 99°C for 10 min, and analyzed by western blotting.

Ubiquitination assay

For detecting endogenous AR ubiquitination in LNCaP cells, 5.0×10^6 cells were grown in a 10 cm dish. Cells were treated with MG132 for 4 h before harvesting at 72 h. Cells were then lysed with RIPA buffer, and whole-cell lysates were immunoprecipitated overnight at 4°C with protein G Dynabeads (Invitrogen) coated with anti-AR antibody or rabbit IgG. The following day, the beads were washed three times with BC300 buffer, once with BC100 buffer, boiled in $2 \times$ SDS-PAGE sample buffer at 95°C for 5 min, and analyzed by western blotting.

Xenograft tumor growth

All mice procedures were approved by the Institutional Animal Care and Use Committee at the University of Macau and complied with all relevant ethical regulations. 3–5 week-old male nude mice were used. To evaluate the role of TRIM33 in tumor formation, 3×10^6 LNCaP cells stably expressing shCtrl or shTRIM33 (purchased from OriGene) were inoculated by subcutaneous injection into the dorsal flank of the mice (the animals were randomly allocated as two groups). Tumor size was measured twice a week, while tumor volume was estimated using the formula $1/2 * (L * W^2)$ (L = the length of the tumor, W = the width). Once the endpoint was reached, mice were euthanized, and tumors were excised and weighed.

Data availability

All the sequencing data from this work have been submitted to the NCBI Gene Expression Omnibus (GEO) under accession number

GSE174590 (<https://www.ncbi.nlm.nih.gov/geo/query/acc.cgi?acc=GSE174590>).

The mass spectrometry proteomics data have been deposited to the ProteomeXchange Consortium via the PRIDE partner repository with the dataset identifier PXD031273 (<http://www.ebi.ac.uk/pride/archive/projects/PXD031273>).

Expanded View for this article is available online.

Acknowledgements

We are grateful for financial support from the University of Macau (MYRG2018-00033-FHS and MYRG2020-00100-FHS) and the Macau Science and Technology Development Fund (102/2015/A3 and 0011/2019/AKP) to EC. We would like to thank Jason Carroll for his advice on RIME analysis. We would also like to thank Lingling Hu and Grace Yanying Guo for their help with animal studies. We would like to acknowledge the Animal Research Core, the Genomics, Bioinformatics & Single Cell Analysis Core, and the Proteomics Core at FHS. This work was performed in part at the high-performance computing cluster (HPCC), which is supported by the Information and Communication Technology Office (ICTO) of the University of Macau. We thank Jacky Chan Hoi Kei and William Pang from HPCC for their support and help.

Author contributions

Mi Chen: Conceptualization; data curation; formal analysis; validation; investigation; visualization; methodology; Writing—original draft; project administration; Writing—review and editing. **Shreyas Lingadahalli:** Data curation; Validation; investigation; methodology; Writing—original draft. **Nitin Narwade:** Data curation; Investigation; visualization; Writing—review and editing. **Kate M K Lei:** Data curation. **Shanshan Liu:** Investigation. **Zuxianglan Zhao:** Data curation; Visualization. **Yimin Zheng:** Visualization. **Qian Lu:** Supervision. **Alexander H N Tang:** Supervision; validation; Writing—review and editing. **Terence C W Poon:** Supervision; Writing—review and editing. **Edwin Cheung:** Conceptualization; resources; data curation; supervision; funding acquisition; investigation; methodology; project administration; Writing—review and editing.

In addition to the CRediT author contributions listed above, the contributions in detail are:

MC, SLin, and EC conceived and designed the project. MC, NN, ZZ, and YZ conducted bioinformatics analysis with guidance from EC. MC, SLiu, KMKL, and SLin performed experiments under the supervision of QL, AHNT, TCWP, and EC. MC, SLin, and EC drafted the manuscript with inputs from all the authors.

Disclosure and competing interests statement

The authors declare that they have no conflict of interest.

References

- Agricola E, Randall RA, Gaarenstroom T, Dupont S, Hill CS (2011) Recruitment of TIF1 gamma to chromatin via its PHD finger-bromodomain activates its ubiquitin ligase and transcriptional repressor activities. *Mol Cell* 43: 85–96
- An J, Wang C, Deng Y, Yu L, Huang H (2014) Destruction of full-length androgen receptor by wild-type SPOP, but not prostate-cancer-associated mutants. *Cell Rep* 6: 657–669
- Aucagne R, Droin N, Paggetti J, Lagrange B, Largeot A, Hammann A, Bataille A, Martin L, Yan KP, Fenaux P et al (2011) Transcription intermediary factor 1gamma is a tumor suppressor in mouse and human chronic myelomonocytic leukemia. *J Clin Invest* 121: 2361–2370
- Bennett NC, Gardiner RA, Hooper JD, Johnson DW, Gobe GC (2010) Molecular cell biology of androgen receptor signalling. *Int J Biochem Cell Biol* 42: 813–827
- Cancer Genome Atlas Research Network (2015) The molecular taxonomy of primary prostate cancer. *Cell* 163: 1011–1025
- Chen CD, Welsbie DS, Tran C, Baek SH, Chen R, Vessella R, Rosenfeld MG, Sawyers CL (2004) Molecular determinants of resistance to antiandrogen therapy. *Nat Med* 10: 33–39
- Cox J, Mann M (2008) MaxQuant enables high peptide identification rates, individualized p.p.b.-range mass accuracies and proteome-wide protein quantification. *Nat Biotechnol* 26: 1367–1372
- Decker KF, Zheng DL, He YH, Bowman T, Edwards JR, Jia L (2012) Persistent androgen receptor-mediated transcription in castration-resistant prostate cancer under androgen-deprived conditions. *Nucleic Acids Res* 40: 10765–10779
- Ding YC, Wu HQ, Warden C, Steele L, Liu XL, van Iterson M, Wu XW, Nelson R, Liu Z, Yuan YC et al (2016) Gene expression differences in prostate cancers between young and old men. *PLoS Genet* 12: e1006477
- Dupont S, Mamidi A, Cordenonsi M, Montagner M, Zacchigna L, Adorno M, Martello G, Stinchfield MJ, Soligo S, Morsut L et al (2009) FAM/USP9x, a deubiquitinating enzyme essential for TGFbeta signaling, controls Smad4 monoubiquitination. *Cell* 136: 123–135
- Dupont S, Zacchigna L, Cordenonsi M, Soligo S, Adorno M, Rugge M, Piccolo S (2005) Germ-layer specification and control of cell growth by Ectoderm, a Smad4 ubiquitin ligase. *Cell* 121: 87–99
- Epstein JI, Egevad L, Amin MB, Delahunt B, Srigley JR, Humphrey PA, Grading C (2016a) The 2014 International Society of Urological Pathology (ISUP) consensus conference on Gleason grading of prostatic carcinoma: definition of grading patterns and proposal for a new grading system. *Am J Surg Pathol* 40: 244–252
- Epstein JI, Zelefsky MJ, Sjoberg DD, Nelson JB, Egevad L, Magi-Galluzzi C, Vickers AJ, Parwani AV, Reuter VE, Fine SW et al (2016b) A contemporary prostate cancer grading system: a validated alternative to the Gleason score. *Eur Urol* 69: 428–435
- Feldman BJ, Feldman D (2001) The development of androgen-independent prostate cancer. *Nat Rev Cancer* 1: 34–45
- Ferri F, Parcelier A, Petit V, Gallouet AS, Lewandowski D, Dalloz M, van den Heuvel A, Kolovos P, Soler E, Squadrito ML et al (2015) TRIM33 switches off Irfn1 gene transcription during the late phase of macrophage activation. *Nat Commun* 6: 8900
- Fong KW, Zhao JC, Song B, Zheng B, Yu J (2018) TRIM28 protects TRIM24 from SPOP-mediated degradation and promotes prostate cancer progression. *Nat Commun* 9: 5007
- Grasso CS, Cani AK, Hovelson DH, Quist MJ, Douville NJ, Yadati V, Amin AM, Nelson PS, Betz BL, Liu CJ et al (2015) Integrative molecular profiling of routine clinical prostate cancer specimens. *Ann Oncol* 26: 1110–1118
- Gregory CW, Johnson RT, Mohler JL, French FS, Wilson EM (2001) Androgen receptor stabilization in recurrent prostate cancer is associated with hypersensitivity to low androgen. *Cancer Res* 61: 2892–2898
- Groner AC, Cato L, de Tribolet-Hardy J, Bernasocchi T, Janouskova H, Melchers D, Houtman R, Cato AC, Tschopp P, Gu L et al (2016) TRIM24 is an oncogenic transcriptional activator in prostate cancer. *Cancer Cell* 29: 846–858
- Gu ZG, Eils R, Schlesner M (2016) Complex heatmaps reveal patterns and correlations in multidimensional genomic data. *Bioinformatics* 32: 2847–2849
- Hatakeyama S (2011) TRIM proteins and cancer. *Nat Rev Cancer* 11: 792–804

- Hatakeyama S (2017) TRIM family proteins: roles in autophagy, immunity, and carcinogenesis. *Trends Biochem Sci* 42: 297–311
- He W, Dorn DC, Erdjument-Bromage H, Tempst P, Moore MA, Massague J (2006) Hematopoiesis controlled by distinct TIF1gamma and Smad4 branches of the TGFbeta pathway. *Cell* 125: 929–941
- He Y, Lu J, Ye Z, Hao S, Wang L, Kohli M, Tindall DJ, Li B, Zhu R, Wang L et al (2018) Androgen receptor splice variants bind to constitutively open chromatin and promote abiraterone-resistant growth of prostate cancer. *Nucleic Acids Res* 46: 1895–1911
- Heemers HV, Tindall DJ (2007) Androgen receptor (AR) coregulators: a diversity of functions converging on and regulating the AR transcriptional complex. *Endocr Rev* 28: 778–808
- Heemers HV, Tindall DJ (2009) Unraveling the complexities of androgen receptor signaling in prostate cancer cells. *Cancer Cell* 15: 245–247
- Heinlein CA, Chang C (2002) Androgen receptor (AR) coregulators: an overview. *Endocr Rev* 23: 175–200
- Heinz S, Benner C, Spann N, Bertolino E, Lin YC, Laslo P, Cheng JX, Murre C, Singh H, Glass CK (2010) Simple combinations of lineage-determining transcription factors prime cis-regulatory elements required for macrophage and B cell identities. *Mol Cell* 38: 576–589
- Herquel B, Ouararhni K, Khetchoumian K, Ignat M, Teletin M, Mark M, Béchade G, Van Dorsselaer A, Sanglier-Cianféran S, Hamiche A (2011) Transcription cofactors TRIM24, TRIM28, and TRIM33 associate to form regulatory complexes that suppress murine hepatocellular carcinoma. *Proc Natl Acad Sci USA* 108: 8212–8217
- Hieronimus H, Lamb J, Ross KN, Peng XP, Clement C, Rodina A, Nieto M, Du J, Stegmaier K, Raj SM et al (2006) Gene expression signature-based chemical genomic prediction identifies a novel class of HSP90 pathway modulators. *Cancer Cell* 10: 321–330
- Hoeller D, Hecker CM, Dikic I (2006) Ubiquitin and ubiquitin-like proteins in cancer pathogenesis. *Nat Rev Cancer* 6: 776–788
- Holmes KA, Brown GD, Carroll JS (2016) Chromatin immunoprecipitation-sequencing (ChIP-seq) for mapping of estrogen receptor-chromatin interactions in breast cancer. *Methods Mol Biol* 1366: 79–98
- Hu R, Dunn TA, Wei S, Isharwal S, Veltri RW, Humphreys E, Han M, Partin AW, Vessella RL, Isaacs WB et al (2009) Ligand-independent androgen receptor variants derived from splicing of cryptic exons signify hormone-refractory prostate cancer. *Cancer Res* 69: 16–22
- Huang DW, Sherman BT, Tan Q, Kir J, Liu D, Bryant D, Guo Y, Stephens R, Baseler MW, Lane HC et al (2007) DAVID Bioinformatics Resources: expanded annotation database and novel algorithms to better extract biology from large gene lists. *Nucleic Acids Res* 35: W169–W175
- Kikuchi M, Okumura F, Tsukiyama T, Watanabe M, Miyajima N, Tanaka J, Imamura M, Hatakeyama S (2009) TRIM24 mediates ligand-dependent activation of androgen receptor and is repressed by a bromodomain-containing protein, BRD7, in prostate cancer cells. *Biochim Biophys Acta* 1793: 1828–1836
- Kim D, Landmead B, Salzberg SL (2015) HISAT: a fast spliced aligner with low memory requirements. *Nat Methods* 12: 357–360
- Kulkarni A, Oza J, Yao M, Sohail H, Ginja V, Tomas-Loba A, Horejsi Z, Tan AR, Boulton SJ, Ganesan S (2013) Tripartite Motif-containing 33 (TRIM33) protein functions in the poly(ADP-ribose) polymerase (PARP)-dependent DNA damage response through interaction with Amplified in Liver Cancer 1 (ALC1) protein. *J Biol Chem* 288: 32357–32369
- Kuner R, Falth M, Pressinotti NC, Brase JC, Puig SB, Metzger J, Gade S, Schafer G, Bartsch G, Steiner E et al (2013) The maternal embryonic leucine zipper kinase (MELK) is upregulated in high-grade prostate cancer. *J Mol Med (Berl)* 91: 237–248
- Langmead B, Trapnell C, Pop M, Salzberg SL (2009) Ultrafast and memory-efficient alignment of short DNA sequences to the human genome. *Genome Biol* 10: R25
- Li B, Lu W, Yang Q, Yu X, Matusik RJ, Chen Z (2014) Skp2 regulates androgen receptor through ubiquitin-mediated degradation independent of Akt/mTOR pathways in prostate cancer. *Prostate* 74: 421–432
- Li H, Handsaker B, Wysoker A, Fennell T, Ruan J, Homer N, Marth G, Abecasis G, Durbin R, Proc GPD (2009) The sequence alignment/map format and SAMtools. *Bioinformatics* 25: 2078–2079
- Li J, Xu CL, Lee HJ, Ren SC, Zi XY, Zhang ZM, Wang HF, Yu YW, Yang CH, Gao XF et al (2020) A genomic and epigenomic atlas of prostate cancer in Asian populations. *Nature* 580: 93–99
- Mansour MA (2018) Ubiquitination: friend and foe in cancer. *Int J Biochem Cell Biol* 101: 80–93
- Massie CE, Lynch A, Ramos-Montoya A, Boren J, Stark R, Fazli L, Warren A, Scott H, Madhu B, Sharma N et al (2011) The androgen receptor fuels prostate cancer by regulating central metabolism and biosynthesis. *EMBO J* 30: 2719–2733
- Miller KD, Nogueira L, Mariotto AB, Rowland JH, Yabroff KR, Alfano CM, Jemal A, Kramer JL, Siegel RL (2019) Cancer treatment and survivorship statistics, 2019. *CA Cancer J Clin* 69: 363–385
- Mills IG (2014) Maintaining and reprogramming genomic androgen receptor activity in prostate cancer. *Nat Rev Cancer* 14: 187–198
- Mohammed H, Taylor C, Brown GD, Papachristou EK, Carroll JS, D'Santos CS (2016) Rapid immunoprecipitation mass spectrometry of endogenous proteins (RIME) for analysis of chromatin complexes. *Nat Protoc* 11: 316–326
- Morrow JK, Lin HK, Sun SC, Zhang S (2015) Targeting ubiquitination for cancer therapies. *Future Med Chem* 7: 2333–2350
- Nelson PS, Clegg N, Arnold H, Ferguson C, Bonham M, White J, Hood L, Lin B (2002) The program of androgen-responsive genes in neoplastic prostate epithelium. *Proc Natl Acad Sci USA* 99: 11890–11895
- Paltoglou S, Das R, Townley SL, Hickey TE, Tarulli GA, Coutinho I, Fernandes R, Hanson AR, Denis I, Carroll JS et al (2017) Novel androgen receptor coregulator GRHL2 exerts both oncogenic and antimetastatic functions in prostate cancer. *Cancer Res* 77: 3417–3430
- Penney KL, Sinnott JA, Tyekucheva S, Gerke T, Shui IM, Kraft P, Sesso HD, Freedman ML, Loda M, Mucci LA et al (2015) Association of prostate cancer risk variants with gene expression in normal and tumor tissue. *Cancer Epidemiol Biomarkers Prev* 24: 255–260
- Pertea M, Pertea GM, Antonescu CM, Chang TC, Mendell JT, Salzberg SL (2015) StringTie enables improved reconstruction of a transcriptome from RNA-seq reads. *Nat Biotechnol* 33: 290–295
- Pickart CM (2001) Mechanisms underlying ubiquitination. *Annu Rev Biochem* 70: 503–533
- Pomerantz MM, Li FG, Takeda DY, Lenci R, Chonkar A, Chabot M, Cejas P, Vazquez F, Cook J, Shivdasani RA et al (2015) The androgen receptor cistrome is extensively reprogrammed in human prostate tumorigenesis. *Nat Genet* 47: 1346–1351
- Ramirez F, Ryan DP, Gruning B, Bhardwaj V, Kilpert F, Richter AS, Heyne S, Dundar F, Manke T (2016) deepTools2: a next generation web server for deep-sequencing data analysis. *Nucleic Acids Res* 44: W160–W165
- Sharma NL, Massie CE, Ramos-Montoya A, Zecchini V, Scott HE, Lamb AD, MacArthur S, Stark R, Warren AY, Mills IG et al (2013) The androgen receptor induces a distinct transcriptional program in castration-resistant prostate cancer in man. *Cancer Cell* 23: 35–47
- Siegel RL, Miller KD, Jemal A (2020) Cancer statistics, 2020. *CA Cancer J Clin* 70: 7–30

- Singh D, Febbo PG, Ross K, Jackson DG, Manola J, Ladd C, Tamayo P, Renshaw AA, D'Amico AV, Richie JP *et al* (2002) Gene expression correlates of clinical prostate cancer behavior. *Cancer Cell* 1: 203–209
- Sung YY, Cheung E (2014) Androgen receptor co-regulatory networks in castration-resistant prostate cancer. *Endocr Relat Cancer* 21: R1–R11
- Tan PY, Chang CW, Chng KR, Wansa KD, Sung WK, Cheung E (2012) Integration of regulatory networks by NKX3-1 promotes androgen-dependent prostate cancer survival. *Mol Cell Biol* 32: 399–414
- Taylor BS, Schultz N, Hieronymus H, Gopalan A, Xiao Y, Carver BS, Arora VK, Kaushik P, Cerami E, Reva B *et al* (2010) Integrative genomic profiling of human prostate cancer. *Cancer Cell* 18: 11–22
- Thorvaldsdottir H, Robinson JT, Mesirov JP (2013) Integrative Genomics Viewer (IGV): high-performance genomics data visualization and exploration. *Brief Bioinform* 14: 178–192
- Vincent DF, Yan KP, Treilleux I, Gay F, Arfi V, Kaniewski B, Marie JC, Lepinasse F, Martel S, Goddard-Leon S *et al* (2009) Inactivation of TIF1gamma cooperates with Kras to induce cystic tumors of the pancreas. *PLoS Genet* 5: e1000575
- Wallace TA, Prueitt RL, Yi M, Stephens RM, Ambs S (2008) Gene expression profiling reveals tumor immunobiological differences in prostate cancer between African-American and European-American men. *Cancer Res* 68: 927–936
- Wang LG, Wang SQ, Li W (2012) RSeQC: quality control of RNA-seq experiments. *Bioinformatics* 28: 2184–2185
- Wang Q, Li W, Zhang Y, Yuan X, Xu K, Yu J, Chen Z, Beroukhim R, Wang H, Lupien M *et al* (2009) Androgen receptor regulates a distinct transcription program in androgen-independent prostate cancer. *Cell* 138: 245–256
- Wei C, Cheng J, Zhou B, Zhu L, Khan MA, He T, Zhou S, He J, Lu X, Chen H *et al* (2016) Tripartite motif containing 28 (TRIM28) promotes breast cancer metastasis by stabilizing TWIST1 protein. *Sci Rep* 6: 29822
- Wisniewski JR (2018) Filter-aided sample preparation for proteome analysis. *Methods Mol Biol* 1841: 3–10
- Xue J, Chen Y, Wu Y, Wang Z, Zhou A, Zhang S, Lin K, Aldape K, Majumder S, Lu Z *et al* (2015) Tumour suppressor TRIM33 targets nuclear beta-catenin degradation. *Nat Commun* 6: 6156
- Yu G, Wang LG, He QY (2015) ChIPseeker: an R/Bioconductor package for ChIP peak annotation, comparison and visualization. *Bioinformatics* 31: 2382–2383
- Zhang Y, Liu T, Meyer CA, Eeckhoute J, Johnson DS, Bernstein BE, Nusbaum C, Myers RM, Brown M, Li W *et al* (2008) Model-based analysis of ChIP-Seq (MACS). *Genome Biol* 9: R137
- Zhu LJ, Gazin C, Lawson ND, Pages H, Lin SM, Lapointe DS, Green MR (2010) ChIPpeakAnno: a Bioconductor package to annotate ChIP-seq and ChIP-chip data. *BMC Bioinformatics* 11: 237